Order Number 9230528

Development and characterization of novel biosensors utilizing plant tissue materials and intact chemoreceptor structures

Wijesuriya, Dayaweera Chandrakantha, Ph.D.

University of Hawaii, 1992

U·M·I
300 N. Zeeb Rd.
Ann Arbor, MI 48106

DEVELOPMENT AND CHARACTERIZATION OF NOVEL BIOSENSORS UTILIZING PLANT TISSUE MATERIALS AND INTACT CHEMORECEPTOR STRUCTURES

A DISSERTATION SUBMITTED TO THE GRADUATE DIVISION OF THE UNIVERSITY OF HAWAI'I IN PARTIAL FULFILLMENT OF THE REQUIREMENTS FOR THE DEGREE OF

DOCTOR OF PHILOSOPHY

IN

CHEMISTRY

MAY 1992

BY

Dayaweera C. Wijesuriya

Dissertation Committee:

Garry A. Rechnitz, Chairperson
Edgar Kiefer
John Head
Che-Chen Chang
William Pong

Dedicated to my parents
for their respect and support of higher education
also to my wife Savi for her love and patience

ACKNOWLEDGEMENTS

The author would like to express his gratitude to Prof. Garry A. Rechnitz for his guidance, encouragement, and patience throughout the years of work on this research, and to the members of the biosensor research group for their thoughtful ideas and discussions. The financial support of the National Science Foundation is greatly appreciated. Finally, the author wishes to express sincere appreciation to his family and friends for their constant support during this period.

ABSTRACT

A biosensor is defined as a device which incorporates a biological component which is either intimately connected to or integrated within a transducer. Plant tissue materials and intact chemoreceptor structures are utilized as molecular recognition elements to construct biosensors with selectivity for various important analytes.

The use of grape tissue as a source of catalase for the determination of hydrogen peroxide was demonstrated. A slice of grape tissue attached to the membrane of a Clark-type oxygen sensor was used to monitor the oxidation of hydrogen peroxide by catalase. Characterization of the novel sensor in terms of selectivity, sensitivity, reproducibility, linear response range and lifetime is reported.

The use of pea seedlings as a source of diamine oxidase for the determination of enzymatic oxidation rates, which are important in evaluating the plant growth-regulating activity, of various amines was investigated. A mixed carbon paste-plant tissue amperometric sensor was constructed and characterized using spermidine as a substrate . Generation of hydrogen peroxide due to enzymatic oxidation of the amine was monitored at 0.9 V vs. Ag/AgCl under steady-state conditions using this sensor. Easy construction, reliability of the data, reusability and shorter response times are some of the advantages of this sensor.

Receptor-based biosensors using chemosensing structures from

fresh-water species (crayfish) are shown to give selective analytical responses to the antitubercular drug, pyrazinamide. The frequency of action potential responses evoked by chemical stimulation of nerve cells was measured using a conventional electrophysiological technique. The construction of such biosensors, in general, is facilitated through the use of a video imaging inverted biological microscope during the manipulation and assembly of the delicate structures involved. Characterization of the novel sensor in terms of selectivity, sensitivity, response time, dose/response relationship, and lifetime is reported. The advantages of using fresh-water versus salt-water species in constructing neuronal biosensors are also discussed.

A reusable neuronal sensor selective to the neurotoxin 3-acetyl pyridine was constructed by using the antennular structure from crayfish. Reusability of the sensor was studied with emphasis on the reproducibility of action potential responses. Characterization of the novel sensor in terms of selectivity, response time and dose/response relationship is reported. The current status of attempts at lifetime extension of neuronal biosensors are discussed.

TABLE OF CONTENTS

LIST OF FIGURES

CHAPTER 1
INTRODUCTION

1.1 DEFINITION OF BIOSENSOR

A biosensor is defined as "an analytical device which incorporates a biological sensing element in intimate contact with, or integrated within, an appropriate transduction element for the purpose of detecting (reversibly and selectively) the concentration or activity of chemical species in any type of samples" (1). The "biological sensing element" has been called a molecular recognition element because it "recognizes" a particular analyte, thereby providing the sensor with a degree of selectivity. The "transduction element" is a device which converts the chemically coded information, received by the molecular recognition element, into a measurable signal.

The most commonly used biological components involve (a) chemoreceptors such as intact structures, and preparations containing isolated chemoreceptors (b) antibodies/antigens such as polyclonal antibodies, monoclonal antibodies, antibody fragments, and enzyme/antigen conjugates (c) biocatalysts such as isolated enzymes, enzyme sequences, microorganisms, and plant or animal tissues. The transducers used may be electrochemical, optical, calorimetric, or acoustic/mechanical (2).

1.2 HISTORICAL DEVELOPMENTS

The evolution of the first biosensor began in the mid-1950s, when Leland C. Clark, Jr., of the Children's Hospital Research Foundation in Cincinnati invented an electrode designed to measure dissolved oxygen (3) in the blood of patients undergoing surgery. The oxygen sensor consisted of a standard platinum electrode and reference electrode with a plastic membrane permeable to gases. The voltage bias of the platinum electrode was set so that the rate of current flow through the circuit depended on the rate at which oxygen diffused through the membrane, which in turn was directly proportional to the external oxygen concentration.

By 1962 Clark had extended the "oxygen electrode" to sense blood glucose levels (4). Glucose oxidase was immobilized at the tip of a Clark pO_2 electrode and the increased O_2 uptake due to enzymatic oxidation of glucose into glucanolactone and hydrogen peroxide was monitored. During the 1960s and early 1970s, numerous biosensors were developed by coupling isolated or purified enzymes to various electrochemical transducers.

Special attention was given to research on bioselective membrane electrodes in the early 1970's when stable and reliable potentiometric sensors for ammonia, carbon dioxide, hydrogen sulfides, and other dissolved gases became commercially available on a routine basis (5,6). Such electrodes combined the technology of ion-selective membrane electrodes with that of pores synthetic membranes.

In the mid 1970's, it was shown that viable whole cells could be collected and kept intact on inert supports such as silica gels and teflon membranes (7). These findings suggested that bacteria and other cells might be used as alternative biocatalysts for biosensor construction.

In 1978, a novel bioselective membrane electrode was constructed by coupling living bacteria of the *Strain Sarcina flava* to a potentiometric ammonia gas sensor for the determination of L-glutamine (8). Essentially, the bacteria functioned as a selective biocatalyst to convert glutamine to other products including ammonia, which produced a change in the measured potential. Tests in aqueous standards and human serum showed that this bioelectrode combined excellent sensitivity and selectivity with rapid response and a useful lifetime of at least 2 weeks. A distinctive feature of bacterial membrane electrodes is the possibility that their lifetimes can be extended through the growth of fresh cells on the electrode surface. This effect has been demonstrated with electrodes for L-asparatate (9) and L-cysteine (10) by using *Bacterium cadaveris* and *Proteus morganii* as biocatalysts, respectively. Shortly after these applications were demonstrated much attention was focused on fabricating other types of whole-cell biocatalysts.

The first bioselective membrane electrode, made with intact animal tissue slices was reported in 1978 (11). This electrode required both beef liver tissue and isolated urease enzyme to mediate the conversion of, arginine, to the electroactive product, ammonia, via two steps:

Arginine ——————> Ornithine + Urea

Urea ——————> CO_2 + $2NH_3$

This electrode demonstrated the concept of using intact tissue slices as biocatalyst even though it suffered from limited utility due to short lifetimes.

A highly effective animal tissue based biosensor selective to, glutamine, was developed by Rechnitz et al. in 1979 (12). By use of a tissue slice from the cortex portion of porcine kidney, which had high level of amino acid deaminase activity, the need for an auxiliary enzyme was eliminated. This tissue-based electrode yielded excellent selectivity, sensitivity, and a much longer useful lifetime than comparable electrodes made with the isolated porcine enzyme while having the additional advantages of simplicity and low cost.

The advantages of using whole cells in place of isolated enzymes include 1) the large supply of fresh biocatalyst within cells and tissues; 2) the ability to use complete, nature-optimized enzymatic path ways; 3) increased stability of the enzyme by maintaining its natural environment; 4) the ability to use biocatalytic activity of enzyme systems which are not available in isolated form; 5) an abundance of necessary co-factors or multi-step reactants; and 6) low cost. However, selectivity is a problem with whole cell based sensors due to the presence of numerous enzymes other than the enzyme of interest.

With the development of other electrochemical techniques such as amperometry and voltametry, tissue slices from animals were coupled

to new transducers for developing biocatalyst based sensors. One such approach was reported by Mascini et al. for the determination of hydrogen peroxide (13), by using a tissue slice from bovine liver as a source of catalase to oxidize H_2O_2 into oxygen and water. Liberated oxygen was measured amperometrically by using Clark style oxygen sensor. This sensor provided several advantages in terms of lifetime, sensitivity, and linear response range over the conventional isolated enzyme-based sensors for the determination of hydrogen peroxide.

Another new class of biosensors were developed in the late 1970 s. Aizawa et al. designed an enzyme "Immunosensor" (14) for the determination of human chorionic gonadotropin (HCG), which is a hormone and an important diagnostic measure of pregnancy. A membrane-bound antibody was used to bind HCG either specifically or selectively on the membrane surface. HCG was labeled using catalase which can decompose H_2O_2 into O_2 and H_2O. Catalase-labeled HCG and non labeled HCG were allowed to competitively react with the membrane-bound antibody of the sensor to form an antigen-antibody complexed on the surface of the membrane. After the removal of nonspecifically adsorbed species, the amount of non-labeled HCG was determined by assaying the catalase activity complexed on the membrane. The membrane-adsorbed catalase enzymatically generated oxygen, when exposed to a H_2O_2 solution, with a resulting increase in the cathodic current of the Oxygen sensor. The initial rate of the

current increase was directly related to the concentration of HCG. A short assay time and its ease of construction are some of the distinct advantages of this method compared to conventional enzyme immunoassay procedures.

1.3 PLANT TISSUE-BASED BIOSENSORS

In the early 1980s, another advance in the development of tissue-based electrode was the discovery that materials of plant origin can be used as effective biocatalyst. In 1981, Kuriyama and Rechnitz created the first plant tissue-based biosensor, utilizing a tissue slice from a yellow squash and a CO_2 electrode (15). The biocatalytic activity of this electrode arose from the glutamate decarboxylase present in the yellow squash tissue. This enzyme breaks down glutamic acid to yield products including CO_2, which is detected by the electrode and produces a potential change related to the concentration of glutamic acid in the sample. This system represented the first successful use of intact plant materials as biocatalysts, in the construction of bioselective potentiometric membrane electrodes. Many plant tissue-based sensors have since been developed utilizing tissue materials from growing portions of plants (e.g. blossoms, young leaves) or their nutrient storage systems (e.g. fruits, seeds, certain vegetables) (16).

1.3.1 RESPONSE CHARACTERISTICS AND LIMITATIONS

The measurement of "steady state" response is the most common technique to obtain useful analytical and kinetic relationships (e.g. calibration plots, response/time curves) for plant tissue-based sensors. At the steady state, rate of diffusion of reactants into the electrode surface is counterbalanced by the rate of diffusion of products away from the electrode. Response of the sensor is plotted against analyte or log analyte concentration, depending on the type of electrochemical transducer employed. However, steady state behavior of such biosensors can be affected by a number of factors including reaction kinetics in the biocatalytic material, concentration of the analyte, and different aspects of the electrode construction. A short range of linear response, slightly over a decade change in substrate concentration, and a relatively high detection limit, typically > 10^{-5} M, are frequently observed with plant tissue-based sensors. The response mechanism for plant tissue-based sensors has not as of yet been determined. In fact, no fundamental studies have been reported concerning the transport mechanism of substrate and product molecules within a tissue slice biocatalyst layer. However, several models have been proposed to describe the interaction between substrate and enzyme within a tissue slice biocatalyst (17).

1.3.2 RESPONSE TIME

The response time of plant tissue-based biosensors primarily

depends upon the tissue thickness used, the tissues inherent enzyme concentration, type of transducer (amperometric or potentiometric electrode) employed, solution pH, temperature, stirring rate, membrane permeability, and analyte concentration. Response times ranging from only a few seconds to several minutes have been reported for various tissue-based biosensors. Theoretically, the thickness of the biocatalyst layer and the effective solution/substrate diffusion constant are the two most important factors in determining electrode response times, as reported by Haneka and Rechnitz (18).

1.3.3 LIFETIME

The working lifetime of biocatalytic membrane electrodes is limited, ranging from less than a day to several months. The relatively short lifetime of tissue electrodes is mainly attributed to the instability of the biocatalyst (tissue materials) employed. The stability of tissue materials is affected by the immobilization technique, storage conditions for the sensor, solution pH, and the presence of activators or inhibitors.

1.3.4 SELECTIVITY

Plant tissue materials very often contain more than one enzyme. Thus, limited selectivity can be expected from tissue-based sensors. However, in some cases excellent selectivity has been achieved especially if the substrate to be determined is a major nutrient or

functional metabolite of the tissue material (16). Although, in principle, isolated enzyme can provide better selectivity than the tissue materials, practical consideration of improved stability, a wider pH working range, and co-factor requirement often favors the use of tissue materials for constructing catalytic biosensors.

1.3.5 METHODS OF IMMOBILIZATION

Immobilization of enzyme biocatalysts is mostly done by cross linking with a bifunctional reagent onto an inert material or alternatively physically retaining the biocatalyst using a suitable membrane. However, with plant tissues the later method was used most often since the biocatalyst is already arranged in an intact structure. The pore size of such membranes needs to be large enough to allow substrate molecules to readily diffuse into the biocatalyst layer in order to undergo catalytic conversion. Therefore, nylon mesh or cellophane dialysis membrane was used earlier to retain the plant tissue at the electrode tip for constructing a biosensor. A long diffusion path through the retaining material often produces slow responses thus its thickness should be kept to a minimum.

1.4 TISSUE-BASED AMPEROMETRIC BIOSENSORS

Research on the use of other transducer types, particularly amperometric, in conjunction with catalytic membranes made from biological materials grew rapidly in the late 1980s. Amperometric

sensors measure an electric current when a voltage is applied between the working electrode and an auxiliary or reference electrode. The chemical specie of interest is either oxidized or reduced at the working electrode. The biocatalyst is used to convert a non-electroactive specie to an electroactive one at the cell voltage selected. The current is proportional to the concentration of the electroactive material present. In addition to the high sensitivity and wide linear range inherent in finite current measurements, amperometric detection offers both great versatility and flexibility allowing for the development of powerful biosensing devices.

1.4.1 MIXED TISSUE-CARBON PASTE BIOSENSORS

In 1988, Wang et al. developed the first "mixed tissue-carbon paste" biosensor by employing the concept of chemically modified electrodes (19). Some of the distinct advantages of this sensor involve fast response, good reusability, ease of miniaturization and feasibility of use in both static and flow systems. The sensor was fabricated by mixing the desired amount of plant tissue into a conventionally prepared carbon paste, made of graphite powder and mineral oil. This mixed biocatalyst-carbon paste electrode substantially reduced the response time due to the absence of a diffusion layer which restricts mass transport. Response of the sensor to variation of analyte concentration is fast since the biocatalyst is an integral part of the sensing element.

At the carbon paste electrode surface, dopamine was converted into

dopamine quinone by the polyphenol oxidase in the banana tissue. Amperometric reduction of quinone at -0.2 V, w.r.t. Ag/AgCl reference electrode was monitored using a flow injection system. Peak height, which is proportional to the current response for the analyte, was plotted against the substrate concentration to obtain an analytical dose/response curve. A detection limit of 20 ng of dopamine could be achieved using this sensor. This type of biosensor construction has recently been applied to the determination of several important analytes by the incorporation of other type of plant tissue materials (20).

New strategies for improving the lifetime and selectivity of plant tissue-based sensors are rapidly being developed. Recently, it has been shown that by substituting plant tissue grown in aseptic culture media the sensor's lifetime is greatly improved. This idea was demonstrated by using a tobacco callus tissue culture to construct a mixed plant tissue-carbon paste electrode for the determination of hydrogen peroxide. The Lifetime of this sensor was over 4 months (21).

1.5 RECEPTOR-BASED BIOSENSORS

The idea that receptors could be incorporated with potentiometric electrodes to produce biosensors was proposed as early as 1975 (22). Neurotransmitter receptor proteins are excellent candidates as sensing elements in biosensors because of their high affinity and selectivity for specific ligands (23,24). They can recognize families of chemicals of

physiological, pharmacological and toxicological significance, that range from amino acids and peptides to therapeutics, drugs of abuse and toxicants. However, the highly complex structures of neuroreceptors, their general labile nature at room temperature, and the difficulty in obtaining sufficient quantities of receptor protein for biosensor studies have restricted attempted biosensor applications of these proteins until recently.

1.5.1 NEURORECEPTORS

Mammalian cells utilize neuroreceptors for the transmission of signals across the lipid membrane that separates the extracellular from the intracellular regions. Neuroreceptor proteins are embedded in the membrane and extend into the adjoining regions, with the specific binding sites for molecular recognition of certain ligands on the extracellular side and signal generators extending into the intracellular region. The general scheme for functioning of neuroreceptors is shown in figure 1, with the main elements consisting of an extracellular ligand binding site and an intracellular signal generator based on either a transmembrane ion channel that opens as a result of ligand binding or a membrane enzyme that undergoes activation or inhibition as a result of ligand binding. The ion channel generated change in concentration of specific ions within the cell can lead to activation or inhibition of intracellular processes; and the change in activity of the membrane enzyme activates secondary messenger systems that in turn govern the

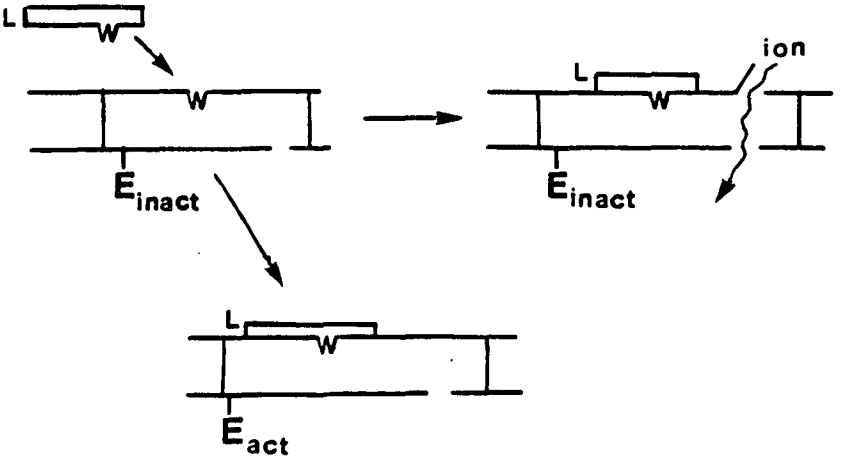

Figure 1. Neuroreceptor functioning, showing ligand L binding to receptor to open ion channel or activate enzyme E.

activities of selective intracellular processes.

1.5.2 NICOTINIC ACETYLCHOLINE RECEPTOR

The nicotinic acetylcholine receptor (nAChR) is the only neuroreceptor for which an alternative natural source exists. The electric organ of the Torpedo Californica electric eel shows high amino acid sequence homology between the nicotinic acetylcholine receptor subunits from the electric eel and those from mammalian skeletal muscle (25,26). Therefore, the nicotinic acetylcholine receptor has become a model for studies of receptor characterization as well as receptor applications, as in biosensors.

The nAChR is made up of five subunits arranged in a circle with a Na^+/K^+ channel in the center of the circle (figure 2) and with each subunit consisting of a sequence of roughly 500 amino acids (subunit molecular weight about 50,000 daltons) (25,26). Four different subunits are present, with the alpha subunit appearing twice in the circle of five subunits that makes up the intact ion channel-binding site receptor complex. The assembled five-subunit complex is thought to have a cylindrical shape about 80 A in diameter by 140 A long, thus spanning the entire 40 A thick bilayer cell membrane and extending well into the extracellular space and also slightly into the intracellular region. The ion channel normally is closed and opens for a few milliseconds only when acetylcholine or other agonist molecules are bound to each of the two alpha subunits. When open, the channel diameter of approximately

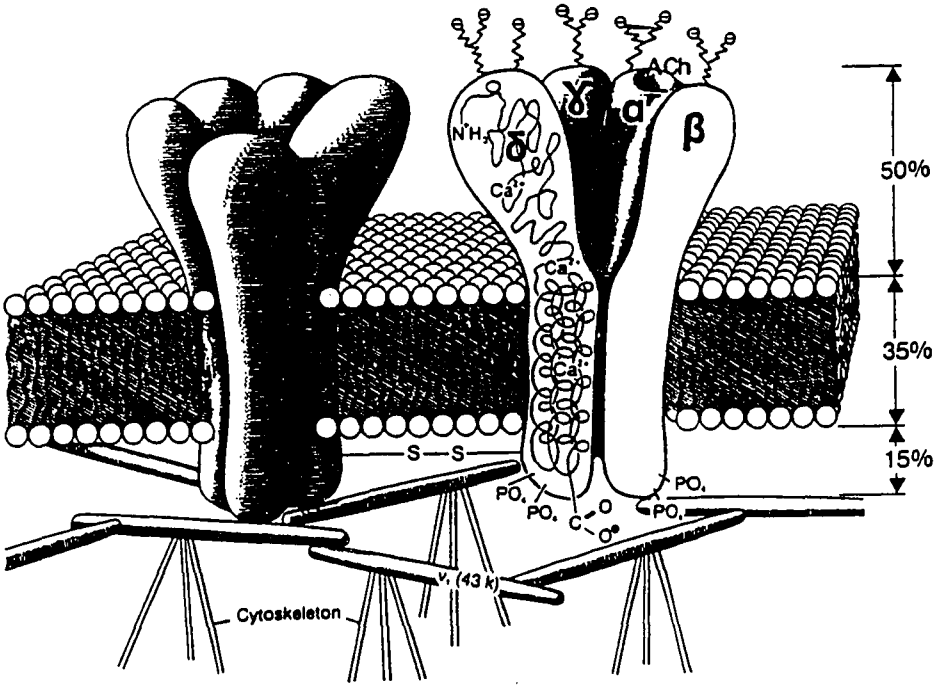

Figure 2. Hypothetical model for the structure of the acetylcholine receptor of *Torepedo californica*.

7 A is sufficient for a hydrated Na^+ ion to pass through.

1.5.3 GABA TYPE A RECEPTOR

The GABA Type A neuroreceptor constitutes another interesting candidate for exploration as a biosensor component. The major features of this receptor system are shown in figure 3 and consist of a chloride ion channel and separate binding sites for GABA (and agonists), benzodiazepines, barbiturates, and toxins such as picrotoxin (27). Only binding of GABA can open the chloride channel; but binding of benzodiazepines or barbiturates at the same time as GABA binding occurs can prolong the duration or frequency of channel opening. The GABA Type A receptor is composed of at least two types of subunits of approximately 50,000 daltons.

Several reports have appeared in which isolated acetylcholine receptors have been utilized with a transducer in attempted demonstrations to recognize selective ligand binding to the receptor. In one attempt, a fixed amount of phenyclidine-labeled enzyme was added to lipid vesicles containing reconstituted acetylcholine receptors (28). Phencyclidine binds strongly to acetylcholine receptors; however the enzyme label was inactivated when the phencyclidine-enzyme moiety bound to the receptor but became active when displaced by free phencyclidine added in an unknown sample. The activity of the enzyme could be calibrated to indicate the concentration of free phencyclidine in the sample. Although this was an innovative method and incorporated

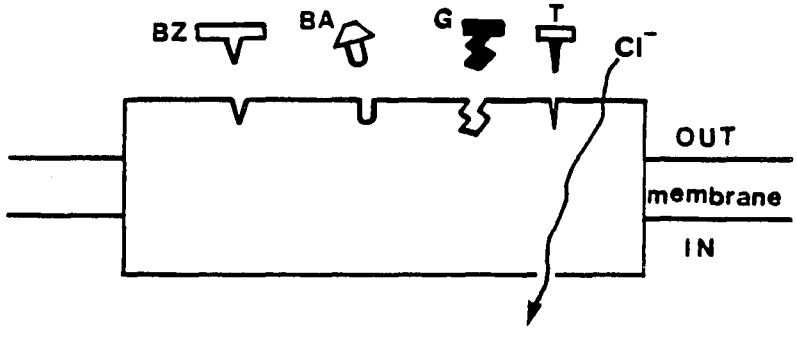

Figure 3. GABA Type A neuroreceptor, showing GABA (G), benzodiazepine (BZ), barbiturate (BA), and toxin (T) binding sites and chloride channel.

an amplification step, the amplification was not carried out through the receptor but through the enzyme label.

In another report acetylcholine receptors were immobilized on the gate of an ion selective field effect transistor (ISFET) (29) by means of 1) a glutaraldehyde-coupled diamine matrix or 2) adsorption in a lecithin (lipid) film. Potentials were measured with respect to a reference ISFET that did not contain the receptor protein. Although this report represented some progress in the evaluation of receptor-based biosensors, in many cases, it is extremely difficult to devise tests to determine the functional integrity of a receptor preparation immobilized on transducers.

Two other reports are available in which AChRs were immobilized by adsorption onto an electrical capacitor (30) and by entrapment or crosslinking in a polymer matrix (31). The occurrence of selective binding was tested by noting a change in electrical capacitance or electrical impedance, respectively. In both cases, it is doubtful that the reported electrical changes could be attributed only to binding of acetylcholine or toxin to the immobilized receptors.

Recently, Rogers et al. developed an acetylcholine receptor-optical biosensor (32), which showed more convincing results for signal generation related to specific binding to the immobilized receptors. In this receptor-optical sensor, the incident light excites a fluorophore just outside the waveguide boundary, then a portion of the resultant fluorescence becomes trapped and is transmitted back up the fiber. This

technique is well suited to a receptor-based or immunochemical biosensor because the fluorescently-tagged ligand, or antibody bound to the receptor protein, which is immobilized at the fiber surface, can be monitored without interference from the ligand in bulk solution.

In general isolated, purified neuroreceptors are labile and need to be stabilized in some manner for use in biosensors. Placing the receptors in an appropriate lipid bilayer, such as a liposome or even a synaptosome would be one route for partial stabilization (33). Another approach would be not to isolate the receptors but to use them in their native environment in tissue slices or in isolated whole cells (34).

1.6 CHEMORECEPTION OF CRUSTACEANS

Sensory receptors of crustaceans fall into two classes, endoreceptors and exoreceptors. The former respond to stimuli arising within the body, the latter to features of the environment or effects occurring at the body surface. Exoreceptors include the organs responsible for the senses of sight, touch, balance, chemo-reception and pressure sense.

Crustaceans have long been known to be able to detect the presence of food at a distance, thus indicating the possession of a chemo-receptive sense. Behavioral experiments suggest that the sense organs responsible for chemo-reception are more widely distributed on the body than those mediating the corresponding smell/taste sense in ourselves. Apart from mouth region, the outer flagellum of the

antennule, the chelipeds and dactylus of the walking legs seem to be well equipped with sensory endings able to initiate behavioral responses to chemical substances (35).

On the outer flagellum of the antennules of crustaceans there are specialized groups of hairs, the aesthetascs, which have been long suspected of chemo-sensing function. These aesthetascs represent the large aggregation of chemoreceptors in these animals. These hairs are arranged in rows and, are thin-walled and unpigmented. Each hair has a large number, perhaps 120-150, of neurons at its base, so that a hair row will contain some, 4000 neurons, and the flagellum as a whole about half a million.

Mechanical stimulation of the hairs does not excite the neurons but they become active in the presence of, for e.g., TMO and betaine. Such a large accumulation of neurons presumably represents a considerable potential for the detection of numerous compounds (36).

1.6.1 CELLULAR ION PUMPS

The membranes of all living cells contain ionic pumps, carriers and ionic channels. Primary ion pumps establish concentration gradients which are an intermediate store of metabolic energy. The subsequent entropic flows of the ions along these gradients drive the antientropic transport of other solutes, such as monosaccharides and amino acid molecules, which are thus actively pumped within the cytoplasm by a secondary active transport. Out of the many types of ions for which

primary ion pumps establish concentration gradients: H^+, Na^+, K^+, Ca^{+2}, Mg^{+2}, Fe^{+3}, Cl^-, HCO^{-3}, only H^+ and Na^+ are found in evolution for driving the secondary active transport of other substances. The H^+-driven active transport occurs in microorganisms and plants, while Na^+ driven flows are specific for animal cells (37).

The ionic pumps, carriers, and ionic channels are particularly well represented and much studied on the epithelial cells (38), whose property is to maintain distinct ionic composition between the compartments they delineate. In the excitable membranes, the ionic channels have the particular feature of being gated, their structure being so that the transition between the closed and the open conformations is triggered by changes in the transmembrane electric field or, in some specialized zones of contact between communicating excitable cells, by the attachment of specific ligands. Thus, what makes cell excitable is the characteristic of its ionic channels to respond to electrical and chemical stimuli by opening in a transistor-like manner.

1.6.2 TRANSMEMBRANE POTENTIAL

Chemo-electrical conversion is quite obvious in the case of excitable cells which generate transient electric currents in response to stimuli. However it occurs - though in less spectacular forms - in all living cells which maintain, at the expense of chemical metabolic energy, steady electric potential differences between the compartments separated by membranes.

The uneven distribution of electric charges in two compartments separated by a membrane gives rise to various kinds of electrical potentials. When the electric field penetrates the whole membrane and can be detected by electrodes introduced in the adjacent bulk solutions, there is a transmembrane potential, while at the boundary between a membrane surface and the corresponding adjacent solution a surface potential can exist. From a thermodynamic point of view, a transmembrane potential is an equilibrium one if the system as a whole attained that state of equilibrium which is possible in the given conditions. Accordingly, an equilibrium potential cannot serve as a source of free energy, unless the conditions are externally changed (39).

1.6.3 RESTING POTENTIAL

The resting potential is the transmembrane electrical potential difference arising as a consequence of the uneven distribution of several ionic species between the cytoplasm and the outside and different permeability characteristics for the various ionic species; it can be detected with intracellular microelectrodes in all cells, as long as they are "alive", i.e. metabolically active, and shows that the system is out of thermodynamic equilibrium.

1.6.4 ACTION POTENTIAL

The attachment of signal molecules to the membrane receptors induces permeability changes which cause transitory modifications of

the resting potential. In excitable cells, specialized for the rapid transmission of electrical signals, an external reduction of the transmembrane potential beyond a given "threshold" value, makes it to continue in a selfmaintained way its decrease and then to change the sign, before returning to the resting value within a few milliseconds. This "action potential" is the basic electrical event underlying both nervous system and muscular activities.

1.7 ANTENNULAR RECEPTRODE

The first "receptrode" was constructed by using an intact chemosensing structure, the antennule, of the blue crab, *Callinectes sapidus* (40). In this approach, receptors remain in their native environment, which has already been optimized for sensing by nature. The chemosensing cells of the antennule serve not only as highly selective and sensitive molecular recognition elements, but also as biological transducers, converting chemical information into electrical impulses in a matter of milliseconds.

As a result of the interaction of the chemical stimulant with the chemoreceptor sites of the sensory structures, a signal is produced consisting of action potential spikes whose frequency is a function of the stimulant concentration. These potential spikes can be displayed on an oscilloscope and the firing frequency is easily determined with automated counting equipment. A dose/response relationship is obtained by plotting the frequency of spikes against the stimulant concentration.

The neuronal response, R, is related to the stimulant concentration, C, by the equation

$$R=R_{max}/[1+(K/C)^n]$$

where K is a constant, R_{max} is the maximum response, and n is the cooperativity factor (a measure of receptor diversity in responding to differing stimuli). For the simplest case, n=1, assuming receptors with identical properties, this equation is identical to the well known Michaelis-Menten equation for enzyme kinetics.

In 1986, Belli and Rechnitz reported fabrication of the first intact chemoreceptor-based sensor (receptrode) utilizing antennular structures from blue crabs (40). This prototype sensor was shown to yield sensitive and selective responses to amino acids in solutions based upon nerve signals from olfactory chemoreceptors at the sensory tip of the antennule. The detection threshold of the sensor was below 10^{-6} molar and the maximum response frequency showed a linear response relationship of over 3 orders of magnitude.

In 1989 further development of this prototype receptor-based biosensor, the determination of some biologically important purine compounds, was reported (41). Replacement of the wire pick up electrode with a glass mini-suction electrode and design changes to the flow cell helped to extend the lifetime of the system considerably.

Another recent report describes the construction of receptrodes which utilize the chemosensing organs of two other species,

Podophthalmus vigil and *Portunis sanguinolentus*. Both are indigenous to the warm Pacific waters around the Hawaiian islands. This demonstrates that "antennular receptrodes" can be constructed from the chemosensing organs of various organisms and are, therefore, not species limited (42). These studies also demonstrated the great potential of "antennular receptrode" sensitive to chemical stimuli (Trimethylamine oxide) several orders of magnitude below the picomolar level and very broad response ranges (10 orders of magnitude or more).

Neuronal receptor-based biosensors differ significantly from other type of biosensors. In many cases biosensors consist of two components: a molecular recognition element which provides certain degree of selectivity to the sensor; and a transducer which converts the chemically coded information received by the molecular recognition element into electrical or optical signal that can be easily measured. In contrast to most biosensors, in which only the molecular recognition is biological, the antennular receptrode uses biological components as both the molecular recognition element and transducer.

The antennular receptor-based biosensor possesses characteristics that are very desirable in a biosensor: a short response time, a high degree of selectivity and sensitivity, a broad dynamic response range, and the ability to respond to a wide variety of analytes which include amino acids, drugs, hormones, toxicants and neurotransmitters etc.

CHAPTER 2

GRAPE TISSUE-BASED ELECTROCHEMICAL SENSOR FOR THE DETERMINATION OF HYDROGEN PEROXIDE

2.1 BACKGROUND

Hydrogen peroxide is an important industrial material, being used for waste water treatment, sterilization and as a source of oxygen. The area of usefulness of H_2O_2 as an antiseptic and disinfecting agent and as a treatment for certain diseases has been known for over 100 years (43,44). Many detailed studies have been made of the bactericidal action of hydrogen peroxide and peroxy compounds against various microorganisms (45). For e.g., hydrogen peroxide is added as an antibacterial agent to milk (46,47), and subsequently removed by adding catalase before the milk is microbiologically transformed into cheese. A substantial number of reports have also been published of the use of H_2O_2 or peroxy compounds for disinfecting and improving the germination of seeds (48). Hence the determination of H_2O_2 is very important in the food industry and other areas.

Hydrogen peroxide is also produced in living organisms. Production of hydrogen peroxide occurs during normal cellular metabolism by enzymes such as glycolate oxidase and D-amino acid oxidase or simply by non-enzymatic or enzymatic dismutation of oxygen. Hydrogen peroxide is also a by-product of oxidation of glucose to gluconic acid:

B-D-glucose + O_2 + H_2O ———> D-gluconic acid + H_2O_2

H_2O_2 ———> H_2O + 1/2 O_2

Hydrogen peroxide can rapidly inactivate the activity of catalase, which in fact decreases the glucose transformation efficiency (49,50,51). It is often proposed that the toxicity of many drugs and chemicals results from excessive generation of O_2^-. and H_2O_2, perhaps by exceeding the capacity of cellular enzyme systems to remove them efficiently. Therefore, hydrogen peroxide is an important operational parameter whose measurement and control is of some interest.

2.1.1 QUANTITATIVE MEASUREMENTS OF H_2O_2

The most commonly employed quantitative procedures (52) for the determination of hydrogen peroxide include: (1) combined gravimetric and volumetric analysis, consisting of titration with permanganate, ceric, or iodide ions of a weighed sample of the solution; (2) volumetric analysis, consisting of titration of a known volume of the sample with reference to a density chart; (3) gasometric analysis, measurement of the quantity of oxygen evolved in the catalytic decomposition of a known quantity of the hydrogen peroxide solution; (4) colorimetric analysis, depending on the intensity of the color developed in a reaction with hydrogen peroxide; and (5) physical procedures, such as direct measurement of the density or refractive index of the solution, when other dissolved materials are absent. Major drawbacks of these

techniques involve interferences, lack of sensitivities, time factors and also expensive reagents. Electrochemical methods, on the other hand, offer an alternative means of determining hydrogen peroxide. As an example, amperometric oxidation of hydrogen peroxide produced during enzyme reactions has been monitored using a platinum electrode (53). However at high potentials other electroactive species such as ascorbic acid may be oxidized. This is a problem with biological and food-based samples unless appropriate sample pretreatment is applied.

Immobilized enzymes are now widely employed in analytical chemistry (54,55). Polyacrylamide gels (56), nylon nets and controlled-pore glass have been used as supporting materials for the immobilization of enzymes. The use of immobilized peroxidase in association with an immobilized electron transfer mediator has also been reported (57). A bio-electrode in which catalase was coupled electrochemically with a collagen membrane has shown a linear response over a fairly large concentration range, although the lifetime was very short (58).

Tissue-based electrodes (59) have shown much better lifetimes than enzyme electrodes; however, interferences due to other enzymes in the tissue sometimes limit the use of such electrodes (60). An electrode obtained by coupling a Clark-type oxygen electrode and a slice of bovine liver was shown to have excellent stability, sensitivity and a better lifetime than immobilized enzyme electrodes for measuring hydrogen peroxide (13).

2.1.2 CATALASE

Catalase is an enzyme which catalyses the decomposition of hydrogen peroxide into water and molecular oxygen. This enzyme is widely distributed in animal and plant tissues and in microorganisms (61). All aerobic bacteria contain catalase, with the possible exception of Acetobactor peroxydans. The results of various experiments led to the following formulation of the mode of action (62) of catalase:

$$4Fe^{+++}_{(catalase)} + 2H_2O_2 \longrightarrow 4Fe^{++}_{(catalase)} + 4H^+ + 2O_2$$

$$4Fe^{++}_{(catalase)} + 4H^+ + O_2 \longrightarrow 4Fe^{+++}_{(catalase)} + 2H_2O$$

H_2O_2 combines and reacts with catalase, the net result being the reduction of ferric catalase to the ferrous form and the oxidation of H_2O_2 to oxygen and water.

Physical and biochemical transformation reflected by number of enzymes during fruit ripening are well documented in literature. An increasing level of catalase during ripening has been reported in grapes, mango and citrus (63).

2.1.3 ORION RESEARCH MODEL 97-08 OXYGEN ELECTRODE

The model 97-08 dissolved oxygen electrode (figure 4) is a polarographic device of the type first described by Clark in 1956 (3). It consists of a pair of polarized silver electrodes and an electrolyte separated from the sample by a gas-permeable membrane. Oxygen

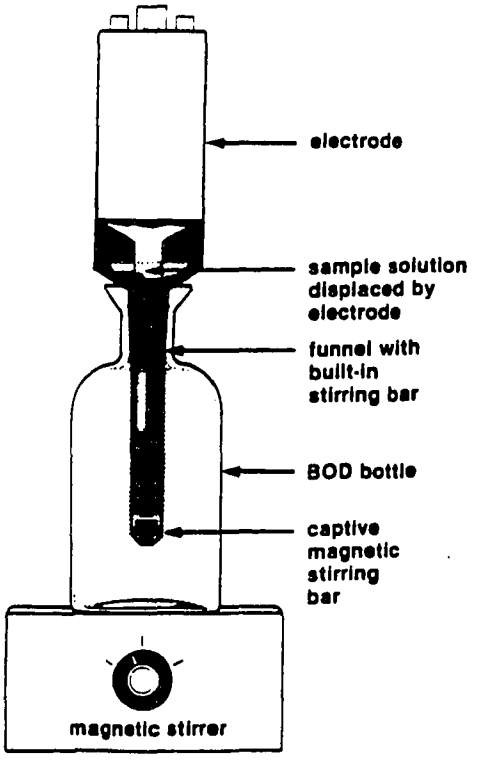

Figure 4. Orion model 97-08 oxygen electrode

diffuses across the electrode membrane and is reduced to hydroxyl ions at a silver cathode according to the reaction:

$$O_2 + 2H_2O + 4e^- \longrightarrow 4OH^-$$

The electrons necessary for this process are provided by a silver anode. Because the electrolyte contains chloride ions, this reaction occurs at the anode:

$$Ag + Cl^- \longrightarrow AgCl + e^-$$

At any given temperature, the current which flows between cathode and anode is directly proportional to the level of oxygen outside of the membrane. Response time of the sensor, t_{96}, is about 30 seconds and the dissolved oxygen concentration within 0-14 ppm can be measured with $\pm$ 0.05 ppm accuracy. Operating temperature range of the sensor could be between 0^0C to 45^0C.

2.2 EXPERIMENTAL

2.2.1 APPARATUS

All measurements were made with an Orion Research Model 97-08 oxygen electrode and Corning pH/mV meter in conjunction with a Linear 1200 strip-chart recorder. A Haake Model FS water-bath with thermostated cells was used to maintain a constant temperature.

2.2.2 REAGENTS AND TISSUE

Analytical-grade reagents and distilled water were used for the preparation of all solutions. A 30% hydrogen peroxide solution was used to prepare more dilute standard solutions. Their molarity was determined by titration with standard potassium permanganate solution. These standard solutions were prepared in 0.1 M phosphate buffer (pH 7.0), except where indicated otherwise. Grape tissue was obtained from Thompson seedless green grapes (*Vitis vinifera*) available in local supermarkets.

2.2.3 ASSEMBLY OF THE GRAPE TISSUE-BASED SENSOR

The physical construction of the grape tissue-based electrode is shown schematically in figure 5. Tissue slices taken from the layer immediately below the skin of green grapes were placed on the sensing membrane of the Model 90-08 oxygen electrode. The tissue was kept mechanically in place by a nylon (100%) net fixed with an O-ring. Tissue electrodes were soaked in phosphate buffer (pH 7) to remove any soluble fractions prior to use. Grape tissues were stored in phosphate buffer (pH 7) at 4^0C when not in use.

2.2.4 PROCEDURE

Responses of the sensor were monitored at 1 X 10^{-4} M hydrogen peroxide concentration in a series of phosphate buffer solutions ranging from pH 4.5 to 8.5. Dissolved oxygen was measured (in ppm) at the

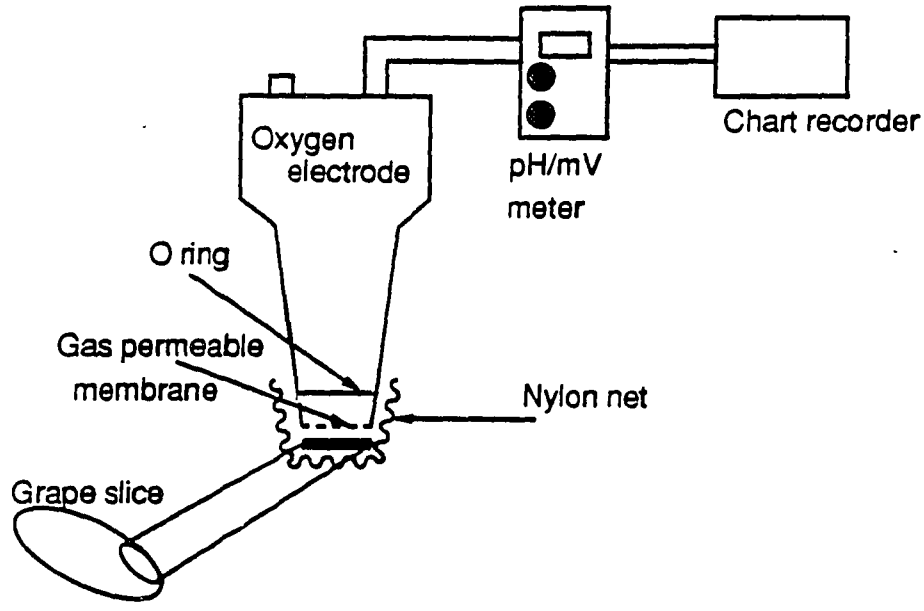

Figure 5. Schematic diagram of the experimental set up.

steady state. For calibration, the response of the sensor due to stepwise addition of hydrogen peroxide (0.01 M) to 10.00 ml of phosphate buffer (pH 7) was recorded on a strip-chart recorder. Phosphate buffer solutions were deaerated with nitrogen before injecting hydrogen peroxide for all the experiments. Response time curves were obtained for step changes in hydrogen peroxide concentration between $5X10^{-5}$ and $1X10^{-4}$ M. The variation of the responses for tissues from different grapes was measured at 0.3 mM hydrogen peroxide. The response of the sensor at 1 mM level of interferents was monitored at $5X10^{-5}$ M hydrogen peroxide. The grape tissue sensor was calibrated over 17 days to study the long-term stability.

2.3 RESULTS AND DISCUSSION

2.3.1 pH STUDIES

Figure 6 shows the variation of response of the sensor with pH at $1X10^{-4}$ M hydrogen peroxide concentration. The mid-pH range from 5.5 to 8.5 is appropriate for good sensitivity. The wide pH range found indicates that the grape tissue sensor will not be subjected to problems arising from external variation in pH. Comparison with the enzyme-collagen hydrogen peroxide sensor (58) shows that the grape tissue electrode is much less sensitive to pH changes. Over the pH range 6-8 the reported current variation for the enzyme electrode was 60% whereas the grape tissue electrode produced responses that varied by only 3% in the pH range 5.5-8.5. Based on these results, phosphate buffer

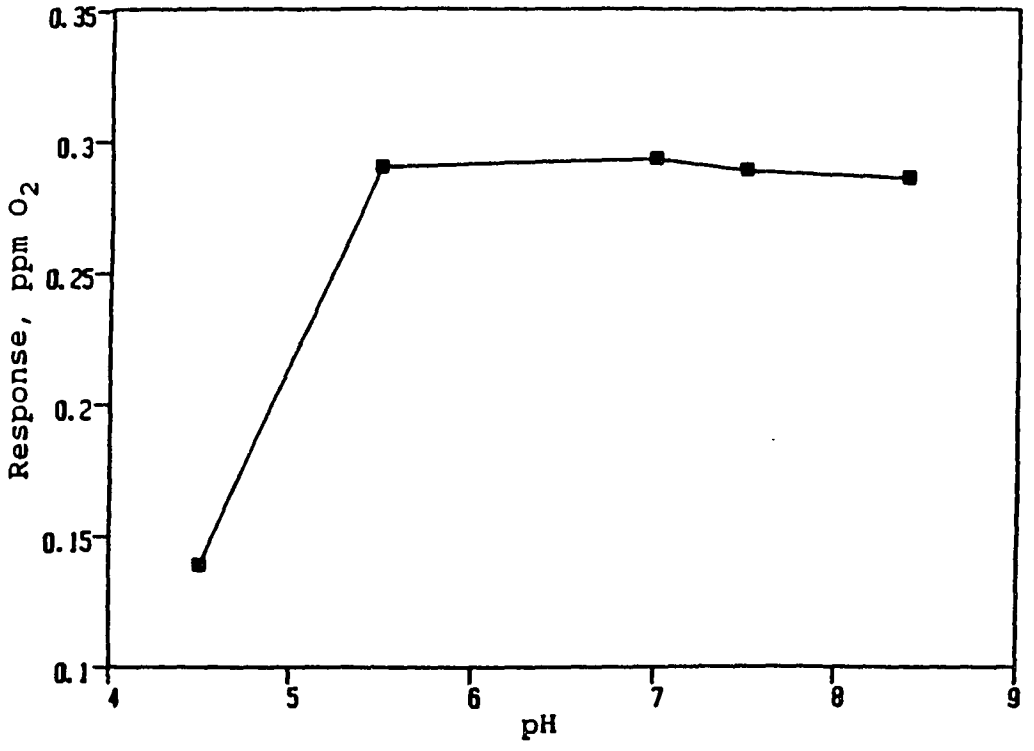

Figure 6. Influence of pH on the output of the sensor for a H_2O_2 concentration at 0.01 mM. Phosphate buffer, 23^0C.

solution of pH 7.0 was used for remainder of the experiments.

2.3.2 RESPONSE TIME OF THE SENSOR

In figure 7, the response characteristics of the sensor are shown for two step changes in hydrogen peroxide concentrations. Phosphate buffer solutions were deaerated with nitrogen initially to minimize the background response. The steady-state response was recorded for the generation of oxygen due to the decomposition of hydrogen peroxide by catalase in the grape tissue. The response time (T_{90}) calculated from the response-time curve was of the order of 1 minute, which is comparable to that of previously reported enzyme-based sensors for hydrogen peroxide determinations (13,58). In general, the response time of the sensor depends on membrane thickness, enzyme concentration, substrate concentration and temperature (58,64). However, the response time studies done with grape tissue sensors indicated no significant change in response time with different thicknesses of the tissue, owing to the high enzyme activity level in the tissue.

2.3.3 CALIBRATION OF THE SENSOR

Figure 8 shows a calibration graph for the grape tissue hydrogen peroxide sensor. Deaeration of the buffer solution prior to calibration improved the detection limit by decreasing the background response. The response of the sensor is linear in the range $1X10^{-5}$ - $5X10^{-4}$ M

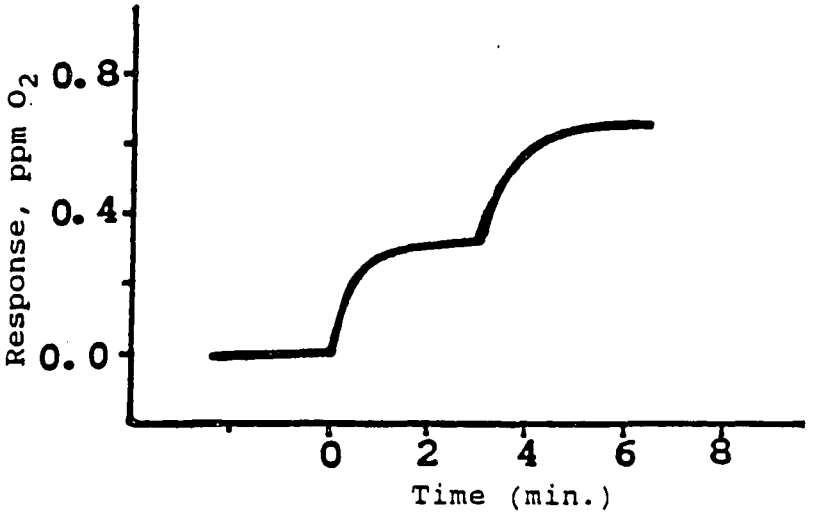

Figure 7. Dynamic response to successive additions of $5X10^{-5}$ and $1X10^{-4}$ M H_2O_2. Phosphate buffer (pH 7.0), 23^0C.

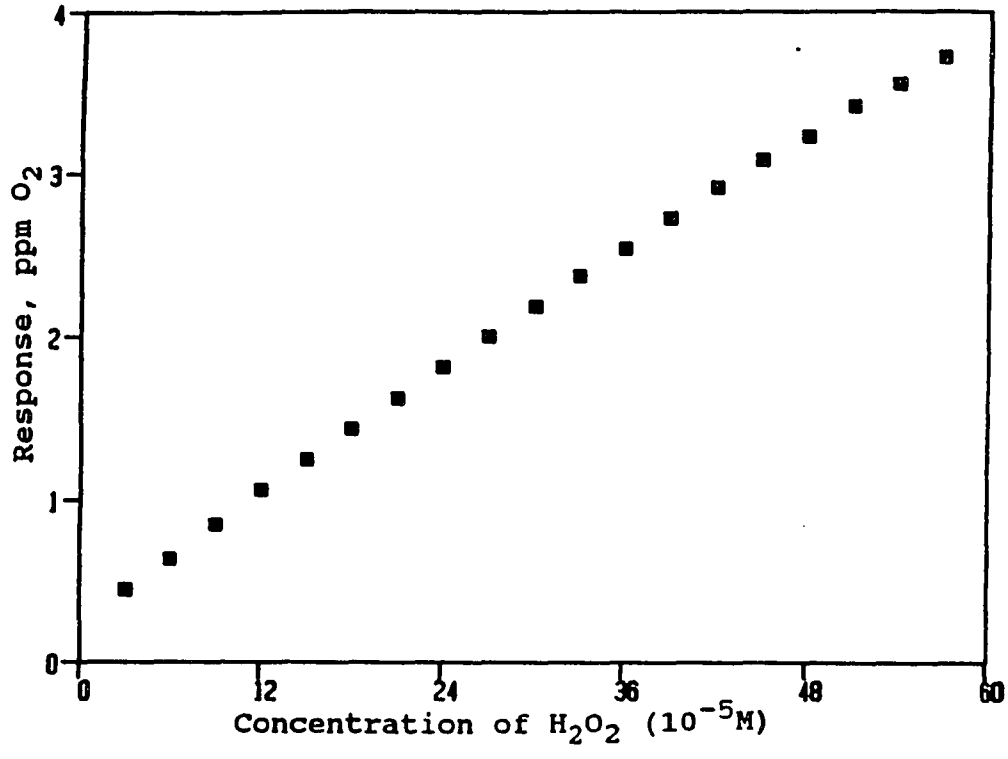

Figure 8. Calibration graph for H_2O_2 in phosphate buffer (pH 7.0) at 23^0C in a solution deaerated with nitrogen.

hydrogen peroxide. The standard error of the estimates, $S_{y.x}$, a measure of the residual variation about the line, was calculated to be 0.094 ppm O_2. This value of $S_{y.x}$ is very small compared with S_y (4.74 ppm), the standard deviation of the y values from the mean of all the y observations (response in ppm O_2), and indicates a good correlation between the response of the sensor and hydrogen peroxide concentration. Higher concentrations of hydrogen peroxide produced unstable results, perhaps owing to poisoning of the tissue or saturation effects, as demonstrated by other workers (58).

2.3.4 REUSABILITY OF THE SENSOR

Repeated calibration of the grape tissue sensor within a single day showed no significant changes in the slope of the calibration graphs. Three calibrations taken within a day, produced 6.44 $\pm$ 0.08, 6.44 $\pm$ 0.51 and 6.40 $\pm$ 0.04 as the slopes (in ppm O_2 mM^{-1} H_2O_2). The variation of responses for tissues from different grapes was monitored at 0.3 mM hydrogen peroxide. The relative standard deviation for eight different grapes was 1.6%, indicating only a slight variation of responses from one grape to another.

2.3.5 INTERFERENCE STUDIES

Many enzymes other than catalase can be expected in the grape tissue and this may limit the selectivity of the proposed sensor. Other

types of substrates can interfere with the system provided that they can change the dissolved oxygen concentration or alter the primary enzyme reaction. However, it was found experimentally that millimolar levels of ethanol, amino acids (such as alanine, methionine, tryptophan and tyrosine), glucose or lactic acid did not interfere at a $5X10^{-5}$ M hydrogen peroxide concentration. Ascorbic acid did interfere by decreasing the steady-state response of the sensor. This may be due to the decrease in oxygen level by enzymes such as L-ascorbate oxidase in the grape tissue:

$$2\ \text{L-ascorbate} + O_2 \longrightarrow 2\ \text{dehydroascorbate} + 2\ H_2O$$

2.3.6 LONG-TERM STABILITY OF THE SENSOR

The grape tissue sensor was calibrated over 17 days to study its long-term stability. Figure 9 shows the variation of the calibration slopes (ppm O_2 mM^{-1} H_2O_2) within this period. The small (<15%) decline in the calibration slopes demonstrates the excellent stability of the grape tissue sensor for measuring hydrogen peroxide. Retaining enzyme activity in the tissue is the key factor for long-term stability. It has been reported that the catalase activity is actually increased during maturation and ripening of grapes (63), which may be the reason for long-term activity of the catalase enzyme in the grape tissue.

The use of preservatives such as sodium azide to prevent bacterial

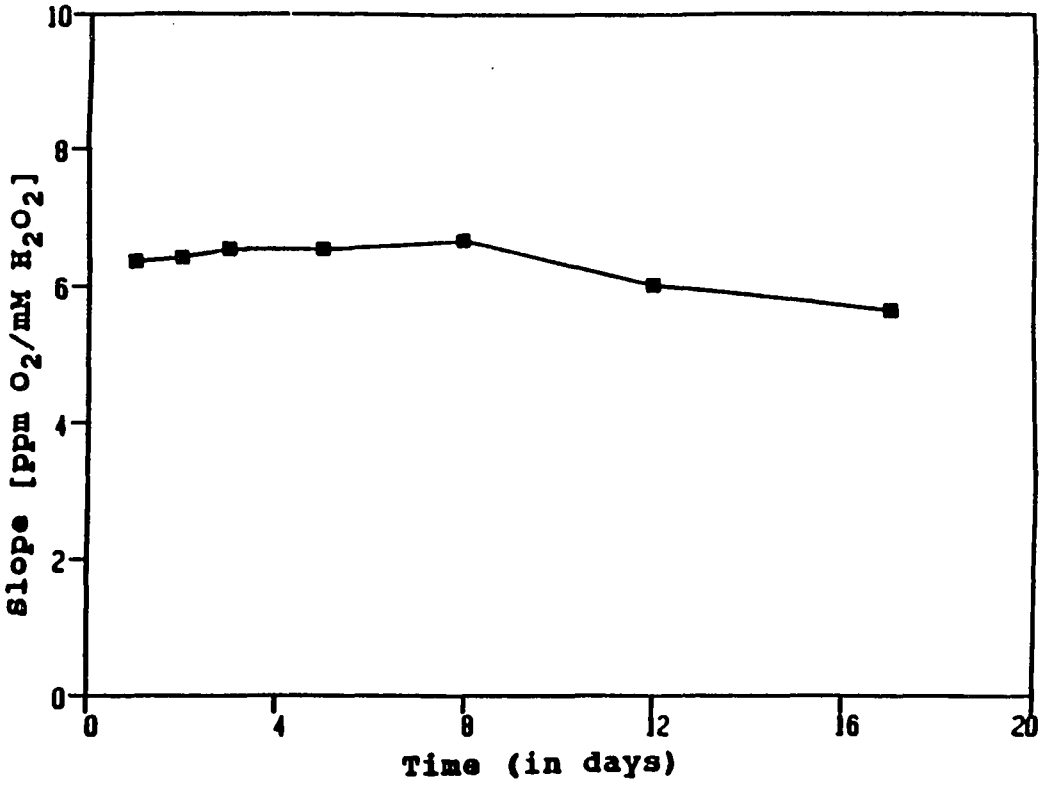

Figure 9. Long-term stability of the grape tissue sensor.

development in the tissue has been reported (13). Grape tissues stored in phosphate buffer (pH 7) containing 0.2% azide showed a marked decrease in response within 3 days, perhaps owing to the inhibition of catalase activity by azide ion, as reported earlier (13). Buffer solution at 4^0C was used to store the immobilized enzyme electrode for several months without a decrease in activity (65). Grape tissues were also stored in phosphate buffer (pH 7.0) at 4^0C when not in use for the long-term stability studies. A distinct advantage of using the grape tissue sensor in measuring hydrogen peroxide is that it can be used for more than 17 days, in contrast to a liver tissue-based hydrogen peroxide sensor, which showed rapid decrease in response within 8 days (13), and a catalase-collagen membrane sensor, which could be used only 10 times (58).

2.4 CONCLUSIONS

The grape tissue sensor described is selective for hydrogen peroxide. It may be used in a simple, rapid and direct method of determining hydrogen peroxide. Repeated utilization of the sensor within a day does not change the calibration slope significantly. This sensor is much less sensitive to pH within the mid-pH range (5.5-8.5) than previously reported sensors. The response of the sensor is linear in the range $1X10^{-5}$ - $5X10^{-4}$ M hydrogen peroxide. The rapid response of the sensor (1 min) is also useful for continuous measurements.

The long-term stability of the grape tissue sensor is much better

than those of previously reported immobilized enzyme and bovine liver-based hydrogen peroxide sensors.

CHAPTER 3

MIXED CARBON PASTE-PEA SEEDLING ELECTROCHEMICAL SENSOR FOR MEASURING PLANT GROWTH-REGULATING ACTIVITY OF AMINES

3.1 BACKGROUND

Plant biochemistry is profoundly disturbed by interaction with herbicides and, in turn, it metabolizes them with accompanying bioactivation or detoxification. Species show considerable differences in their capacity to metabolize herbicides; in many cases, a significant difference in metabolic activity parallels the difference in response between resistant and susceptible species. The biochemical mechanisms involved (66) are strikingly similar to those which have been established in animal tissues for drug metabolism (67), including oxidation affording hydroxylation of aliphatic chain and aromatic ring compounds, oxidative deamination, O- and N-dealkylations, N-oxidation, and sulphoxidation. In addition, plant-peroxidase-mediated oxidative reactions and B-oxidations have been established, together with the reduction of nitro groups and the hydrolysis of esters, lactones, amides, and halogeno substituents. Conjugations with cysteinyl peptides and other thiols and with amino acids, and glycosidations, as well as conjugation involving acylation processes , have been established. As the metabolism of herbicides depends on the type of herbicides and plants employed, it is not feasible to design a sensor for testing the

herbicidal activity of all these herbicides.

3.1.1 PLANT DI-AMINE OXIDASE

Enzymes which oxidize diamines occur sporadically throughout the plant kingdom (68,69), though they are particularly active in the Leguminosae. The diamine oxidase found in pea seedlings (70,71) (*Pisum sativum*) has been purified to homogeneity and shown to contain copper which can be readily removed from the enzyme by dialysis against chelating agents, with consequent inactivation. All plant DAOs studied so far are dimers. Several have been shown to contain two copper atoms and one carbonyl residue per mol of enzyme (72).

Pea seedlings are the most active source of DAO, exceeding the classical hog kidney by 105 times in terms of crude material, and by 58 times in terms of purified enzyme (73). Moreover, the pea seedling enzyme is very stable during long-term storage and in assay. For these reasons the pea seedling DAO may be utilized for estimating amines. Within the Leguminosae, DAOs with properties similar to those of the pea seedling enzyme have been found in other plants such as, Arachis hypogea (74), Glycine max (75), Lens esculenta (76) etc.

The following reactions are typical of those catalyzed by DAO:

putrescine + O_2 ——————> pyrroline + NH_3 + H_2O_2

spermidine + O_2 ——————> aminopropylpyrroline + NH_3 + H_2O_2

The pea seedling DAO is most active with putrescine and cadaverine as substrates (optimum pH 7) though the K_m for spermidine is $5X10^{-6}$ M, smaller than the K_m for putrescine ($4X10^{-5}$ M) (77). The pea seedling enzyme oxidizes a wide range of substrates including aromatic and aliphatic monoamines (78), and lysine and ornithine are also slowly oxidized.

In the pea seedling, DAO is found predominantly in the cotyledons, and activity reaches a peak at 6-16 days after germination in the dark (70). No activity could be detected in the resting seed. Treatment of the seed before germination with putrescine, spermidine or ornithine caused a considerable increase in DAO activity in the cotyledons, suggesting that the enzyme is inducible (79).

3.1.2 HERBICIDAL ACTIVITY OF AMINES

In vitro, enzymatic oxidation rates of amines which are structurally related to plant growth-regulating substances by diamine oxidase (E.C. 1.4.3.6) isolated from pea seedlings have been shown to be a critical factor in determining the herbicidal activity of the amines investigated (80). Amines with higher oxidation rates were more effective than others as herbicides. Hence it is very important to have a convenient and reliable method for monitoring the enzymatic oxidation of such amines prior to use.

That amines, which are structurally related to plant growth

regulators, can be enzymically converted to the corresponding acid is well established (81,82). The oxidation of a series of amines capable of forming potential plant growth-regulating substances has been studied by using pea seedling DAO, and several of these amines were shown to have herbicidal activity in tomato and bean plants (80). The initial reaction, which involves the oxidation of the amines to the aldehyde, is catalyzed by an amine oxidase enzyme (81).

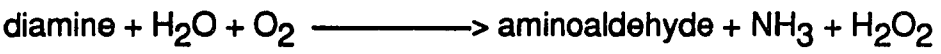

When isolated from pea seedlings, this enzyme shows broad specificity, but there can be differences in oxidation rates between substrates (83). When considered together with the growth-regulating activity of the acid ultimately produced, these rates permit an assessment of the amine as a hormone-type herbicide to be made (80). It has been shown that the rate at which the amine is enzymatically oxidized can be a critical factor in determining its herbicidal activity. However, other factors are also important when predicting the activity of the amine from its oxidation rates. For example, the physical properties of the molecule itself (liphophilic-hydrophlic balance) could affect its penetration and movement within the tissue and the physical properties of the first product of amine oxidation, in this instance the corresponding aldehyde, might also operate in relation to the final activity shown. However, it has been reported that in vitro, enzymic oxidation rates are more important in evaluating the level of herbicidal

activity of the type of aromatic amines studied (80), regardless of the significance of such factors.

3.1.3 OXIDATION RATE MEASUREMENTS

Previous methods for measuring the oxidation rates of amines by the enzyme diamine oxidase involved the use of the fluorescent dye scopoletin (7-hydroxy-6-methoxy-2H-benzopyran-1-one) and horseradish peroxidase (HRP) (80). Hydrogen peroxide generated from the oxidation of amines reacted with scopoletin, which is a substrate for HRP, thus decreasing the fluorescence intensity. A spectrofluorimeter was used to monitor the variation of fluorescence intensity with time. Thus, for any fixed interval of time, the amount of hydrogen peroxide generated could be measured. A number of reducing substances are capable of competitively inhibiting the oxidation of scopoletin by peroxidase (84); for example, ascorbic acid, glutathione and manganous ions. Thus, it is important to remove any interfering substances by a preliminary oxidation, before measuring H_2O_2.

Two other methods of monitoring the oxidation of amines by pea seedling extract involve (85) the colorimetric determination of H_2O_2 by using benzidine as a substrate and the manometric detection of the increased O_2 uptake during the oxidation of amines. The blue coloration obtained when benzidine and H_2O_2 are added to most plants and animal tissues is known to be due to the oxidation of benzidine by peroxidase or

to the peroxidase-like action of haem or haematin derivatives. Therefore, a blue coloration obtained with tissue and benzidine in the absence of added H_2O_2 suggested the formation of H_2O_2 by the tissue. A quantitative study has also been made of the total O_2 uptake (85) during the oxidation of amines and of the products of oxidation. The results obtained depended on whether the extract or the dry preparation of enzyme was used to catalyze the reaction.

A new approach for the construction of tissue-based amperometric bioelectrodes, based upon incorporating the biocatalyst into a carbon paste matrix was described recently (19). The most important advantage of the "mixed biocatalyst-carbon paste electrode" is the substantial reduction of response time owing to the absence of a layer that hinders mass transport. The biocatalyst is an integral part of the sensing element, and hence the electrode responds rapidly to changes in the level of the substrate.

Incorporation of the tissue material from the cotyledon of pea seedling into a carbon paste matrix provided a very reliable sensor for monitoring the oxidation of various amines. As reported earlier (80), in vitro enzymic oxidation rates of amines can be useful in predicting the level of herbicidal activity shown by aromatic amines of the types studied. Responses towards different plant growth-regulating substances can be tested easily with this type of mixed carbon paste-plant tissue system. Generation of hydrogen peroxide due to the

oxidation of amines can be determined amperometrically in this method. Characterization of the sensor was carried out using spermidine as a substrate (K_M=5X10^{-6} M). pH stability, thermal stability, response time, linear range, reproducibility, detection limits, oxidation rate measurements and long-term stability of the sensor are reported.

3.2 EXPERIMENTAL

3.2.1 APPARATUS

A CV-1B voltammograph was used in connection with the three-electrode system for amperometric measurements. A platinum wire and Ag/AgCl electrode were used as counter and reference electrodes, respectively. The working electrode consisted of a mixture of carbon powder, mineral oil and plant tissue. A Polytemp-type water bath with thermostated cells was used to maintain a constant temperature. A linear Model 1200 strip-chart recorder was also connected to the CV-1B to monitor the current response. A schematic diagram of the experimental set up is given in figure 10.

3.2.2 REAGENTS AND TISSUE

Analytical-reagent grade reagents and distilled water were used for the preparation of all solutions. Spermidine trihydrochloride, tyramine hydrochloride, putrescine dihydrochloride and spermine tetrahydrochloride were purchased from Sigma. Standard solutions of spermidine were prepared in 0.1 M phosphate buffer (pH 8.5), except

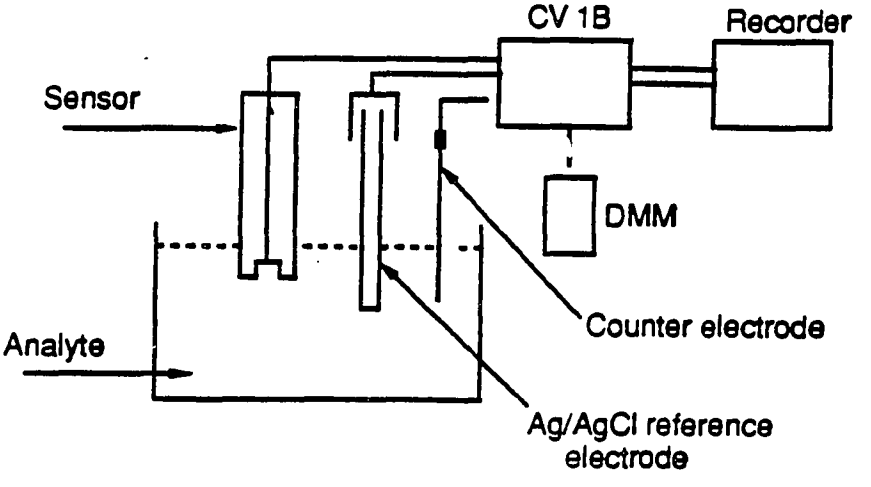

Figure 10. Schematic diagram of the experimental set up.

where indicated otherwise. Wando-type pea (*Pisum sativum*) seeds were bought from a supermarket and soaked for 24 hours in water prior to sowing. Pea seedlings were grown in the dark for appropriate lengths of time. Tissue materials were obtained from the cotyledon of pea seedlings.

3.2.3 PREPARATION OF CARBON PASTE

Appropriate amounts of graphite powder and mineral oil were mixed together to make unmodified electrodes. Different amounts of tissue from the cotyledon of pea seedlings were mixed with the above carbon paste mixture to make modified carbon paste electrodes.

3.2.4 CONSTRUCTION OF THE SENSOR

The cavity of the carbon paste electrode was packed tightly with the carbon paste mixture and smoothed by polishing the tip of the electrode on oil paper. Electrodes were soaked in phosphate buffer solutions for 1 hour prior to measurements. Electrodes and carbon paste mixtures were stored at 0^0C when not in use.

3.2.5 PROCEDURE

Responses of the sensor were monitored at 5 micromoles/liter spermidine concentration in a series of phosphate buffer solutions ranging from pH 4.5 to 9.0. Current due to the oxidation of generated hydrogen peroxide by carbon paste modified electrodes at 0.9 mV vs.

Ag/AgCl was monitored on a strip-chart recorder. Steady-state responses were measured for all the experiments. The response of the sensor was also recorded at 5 micromoles/liter spermidine concentration at different temperatures ranging from 14 to 35^0C to evaluate the thermal stability. For calibration, the response of the sensor to stepwise addition of spermidine (1 mM) to 10.00 ml of phosphate buffer (pH 8.5) was recorded. The response of the electrode for ten replicate measurements at 5 micromole/liter spermidine was also obtained. Response-time curves (current vs. time) were obtained for step changes in spermidine concentration from 2.5 to 5 micromoles/liter. Response-time curves were also obtained for equimolar concentrations (1 mM) of spermidine, putrescine, tyramine and spermine in order to compare the initial oxidation rates. The pea tissue sensor was calibrated over 20 days for studying the long-term stability of the sensor. All experiments were performed at 26^0C except when measuring thermal stability.

3.3 RESULTS AND DISCUSSION

Responses observed from a series of carbon paste modified electrodes containing 6% (w/w) tissues from pea cotyledons ranging from 6 to 10 days in age showed only slight variation of enzyme activity with the age of the seedlings. No enzyme activity was shown from the cotyledons of 1-4-day-old pea seedlings. These results were in agreement with the previously described enzyme assay of pea seedlings

(85). Next, 6-day-old cotyledons of pea seedlings were used to make carbon paste modified electrodes for the remainder of the experiments. In order to establish the optimum amount of plant tissue needed to be mixed with the carbon paste, several modified electrodes were made by varying the percentage of tissue in the carbon paste matrix from 5 to 10% (w/w). Unmodified carbon paste mixture contained 55% graphite powder and 45% mineral oil. The response of this set of electrodes towards 5 micromoles/liter substrates showed 6% tissue to be the optimum; 8-10% (w/w) tissue in the carbon paste matrix produced a high background current response, thus reducing the sensitivity of the sensors, and carbon paste containing 6% tissue from cotyledons of 6-day-old pea seedlings were used for the remainder of the experiments.

3.3.1 pH STUDIES

Figure 11 shows the variation of the response of the sensor with pH at 5 micromoles/liter spermidine concentration. The highest sensitivity was observed near pH 8.5. The sensitivity of the sensor decreased rapidly below pH 7.0 and, in fact, no response was shown below pH 6.0, indicating that the enzyme system in the pea cotyledon is inactive in acid media. The noise level was increased considerably in the more basic medium. The optimum pH of 8.5 for the enzyme system in pea cotyledons is also in agreement with the previously reported data (77). However, according to the enzyme assay procedure given in the

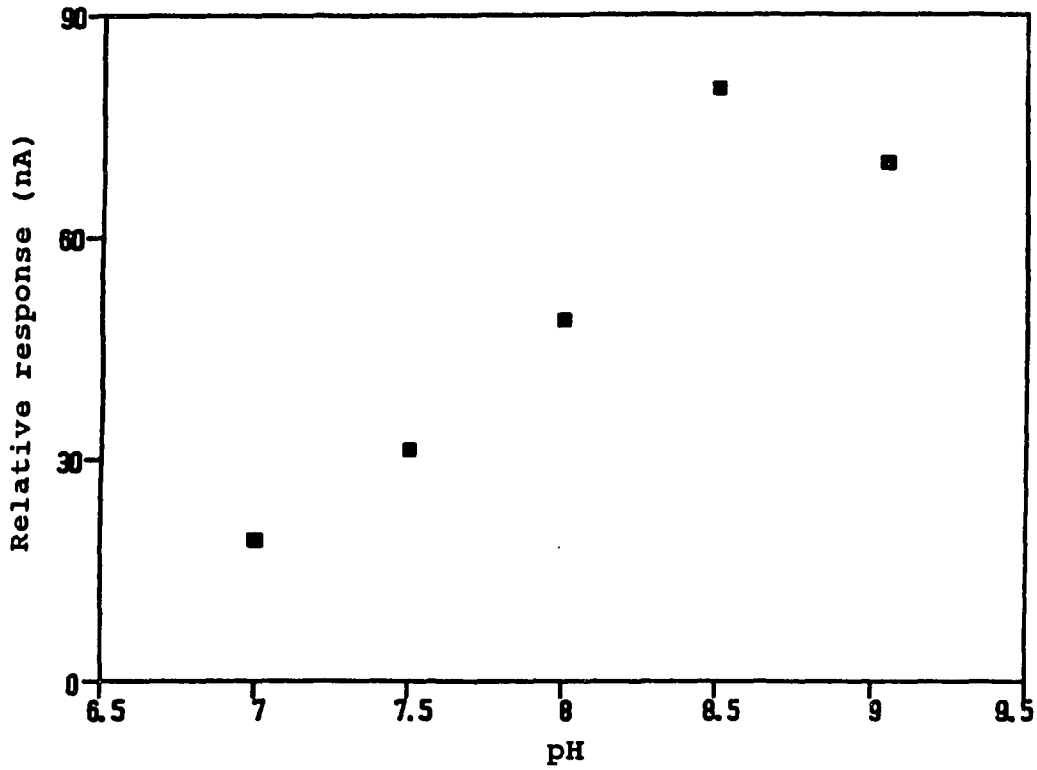

Figure 11. Influence of pH on sensor response for a spermidine concentration of 5 micromoles/liter. Phosphate buffer, 26^0C.

literature (85), the optimum pH of the pea seedling enzyme system is substrate dependent. Thus, for testing any other substrates, pH optimization needs to be done prior to measurements.

3.3.2 THERMAL STABILITY OF THE SENSOR

As shown in figure 12, the response of the sensor was increasing even beyond 35^0C. The significant increase in noise level above 30^0C reflects the instability of the system. Replicate measurements of the response at 5 micromoles/liter at 35^0C produced 85.4 ± 3.2 nA (n=3), indicating that even at high temperatures enzyme activity is retained in the tissue regardless of the noise level. The heat tolerance capacity as seen in this study is in accord with the type of pea seeds used in this experiment. Pea seeds grown in these experiments were recommended for areas with short spring weather where the other varieties were burn out. Because of the excellent heat tolerance capacity, various types of plant growth regulators can be tested under natural growth conditions using this type of sensor. Even for the plants grown in areas where the temperature falls between 14 and 25^0C, the herbicidal activity of amines can also be tested using this type of sensor prior to spraying. Based on these data, all other experiments were done at 26^0C.

3.3.3 RESPONSE TIME OF THE SENSOR

In figure 13, the response characteristics of the sensor are shown for two step changes in spermidine concentration. The steady-state

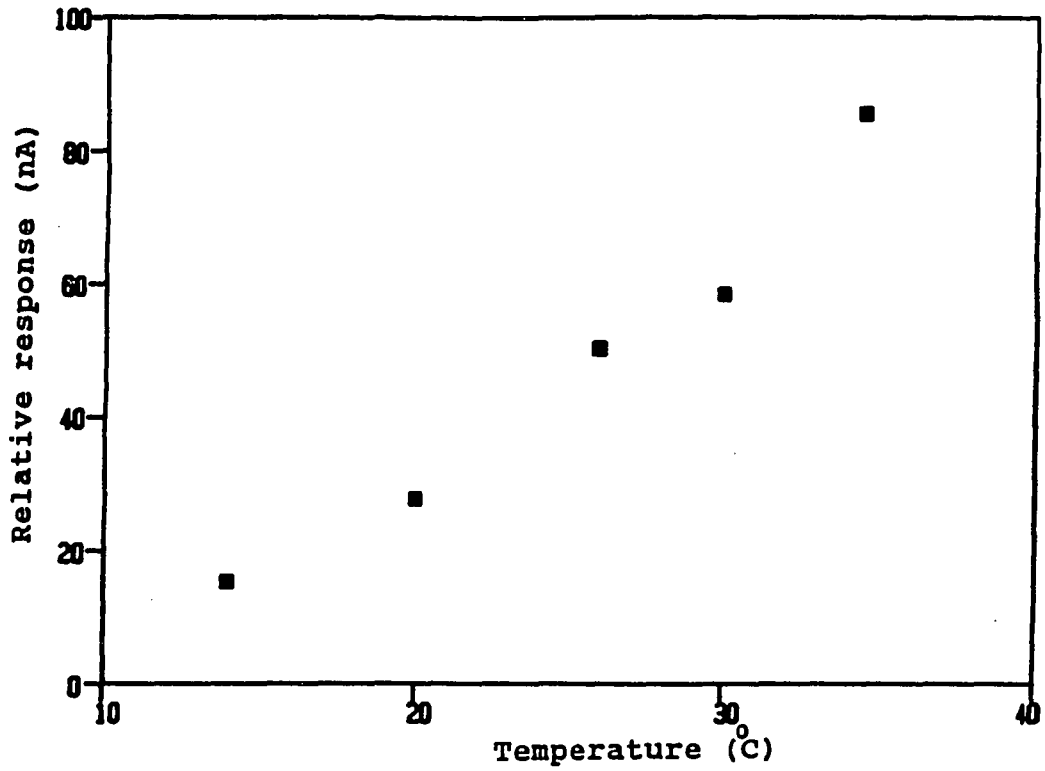

Figure 12. Effect of temperature on the response of the sensor at 5 micromoles/liter spermidine concentration.

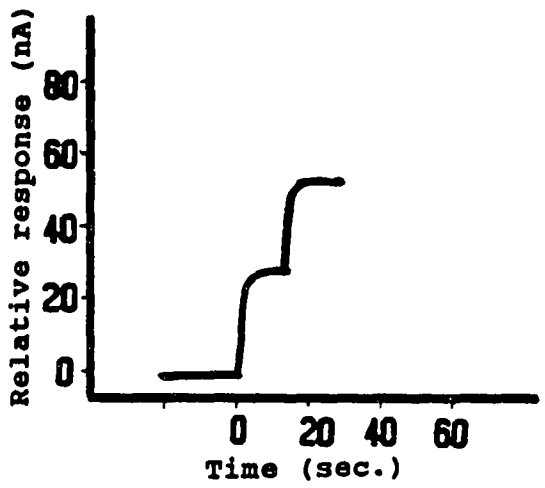

Figure 13. Dynamic response to successive addition of 2.5 and 5.0 micromoles/liter spermidine.

current response was recorded for the oxidation of hydrogen peroxide generated from enzymatic conversion of spermidine in the presence of O_2 and H_2O. The response time (t_{90}) calculated from the response-time curve was ca. 4 seconds, which is much better than those of conventional plant or animal tissue-based biosensors reported previously (86). Diffusion of the substrate into the carbon paste matrix is not necessary because the catalytic reaction takes place at the carbon paste-solution interface. Hence the rate of oxidation depends primarily on the type of substrate used. The slope of the response curves for different substrates at t=0 $[(di/dt)_{t=0}]$, where i and t represent current response and time, respectively, is a good estimate for comparison of the oxidation rates of various amines. The shorter response time of the carbon paste electrode system can also be useful in continuous-flow systems for routine analysis.

3.3.4 CALIBRATION AND REPRODUCIBILITY OF THE SENSOR

Figure 14 shows a calibration graph for the pea seedling-carbon paste sensor towards spermidine. The response of the sensor was rectilinear in the range 0.5 - 4 micromoles/liter spermidine. The standard error of the estimate, $S_{y.x}$, a measure of the residual variation about the line, was calculated to be 1.9 nA. The value of $S_{y.x}$ is very small compared with S_y (43.1 nA), the standard deviation of the y values from the mean of all the y observations (current response in nA),

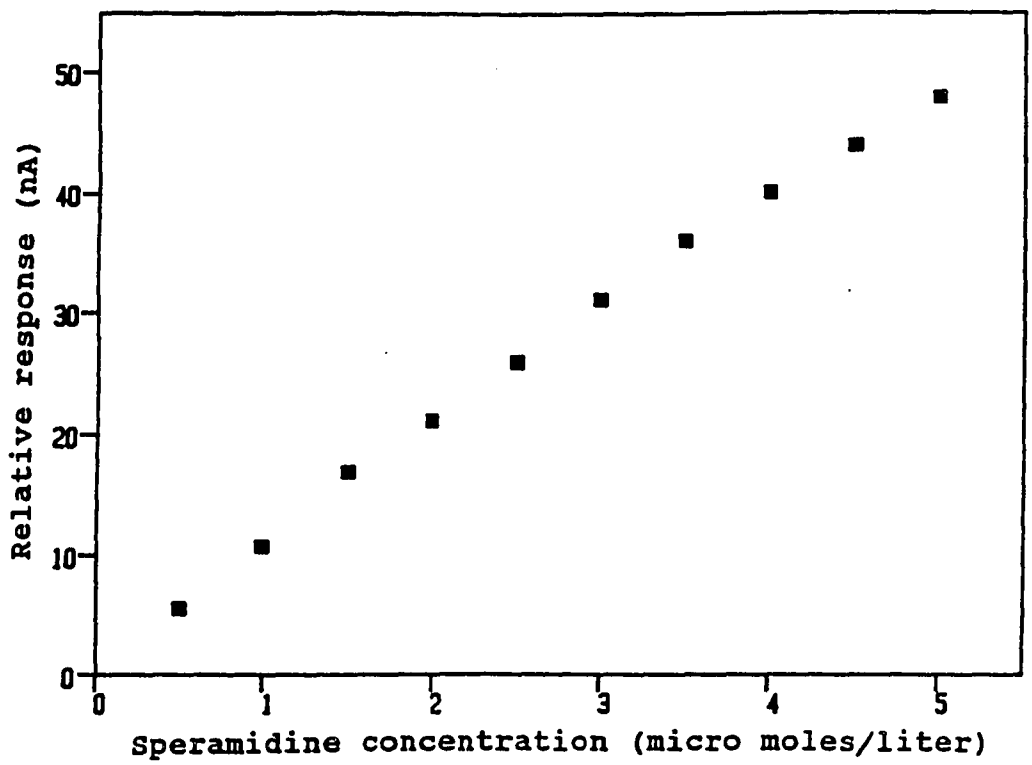

Figure 14. Calibration graph for spermidine in phosphate buffer (pH 8.5) at 26^0C.

and indicates a good correlation between the response of the sensor and spermidine concentration. The detection limit of the sensor was calculated to be 7.1 nmol/liter based on these results. The response of the sensor decreased rapidly at concentrations above 5 micromoles/liter, as expected from the low K_M value of spermidine ($5X10^{-6}$ M). The reproducibility of the sensor was tested by replicate measurements of the response at 5 micromoles/liter spermidine concentration. As shown in figure 15, the variation of the response is negligible for ten replicate measurements, indicating good reproducibility of the sensor.

3.3.5 MEASUREMENT OF OXIDATION RATES

Rates of oxidation of amines $[(di/dt)_{t=0}]$ were calculated from the corresponding response-time curves obtained for four different substrates. The oxidation rates increased in the order spermine< tyramine< putrescene< spermidine, indicating a good correlation with previously reported data (85). Triplicate measurements of oxidation rates for each substrate followed the same order as above. Two conventional methods were applied to monitor the oxidation of plant growth-regulating amines by enzymes in pea seedlings. The first involved the use of horseradish peroxidase in spectrofluorimetric detection (82,84) and the second was based on the manometric detection of oxygen consumption during the oxidation of amines (85).

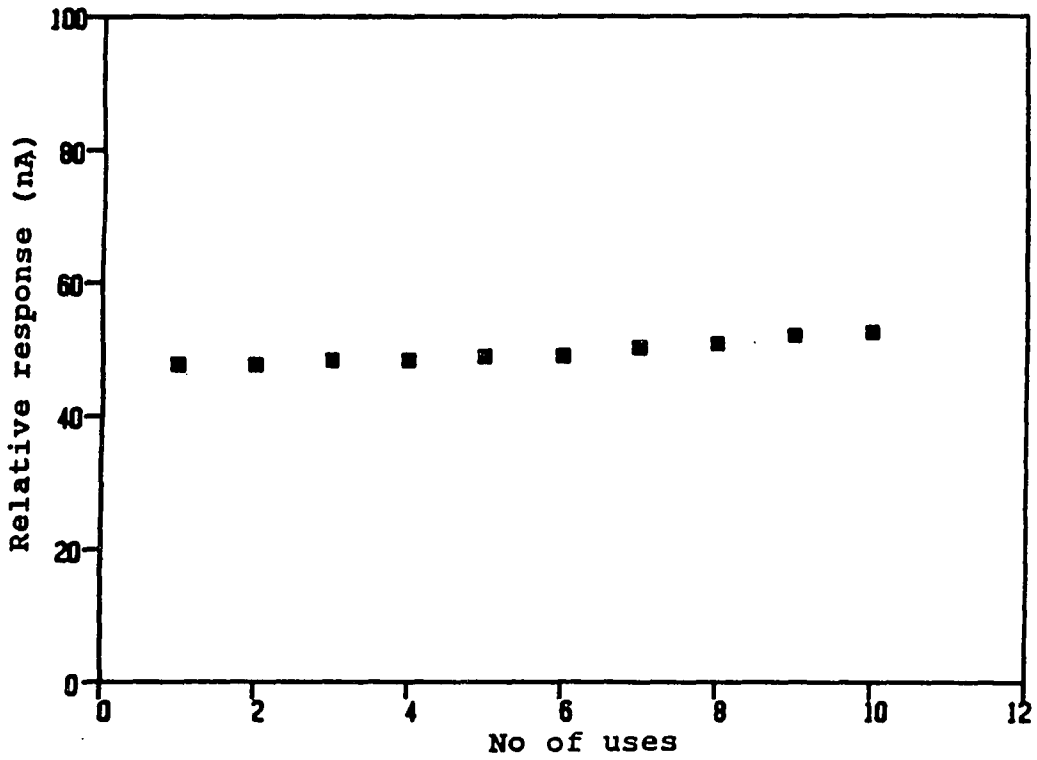

Figure 15. Sensor response with repeated use at 5 micromoles/liter spermidine.

The reproducibility of the data obtained with manometric detection of oxygen consumption was not satisfactory. Even with the fluorescence detection, extraction of the enzyme system is necessary prior to the addition of amines. Isolation of enzyme from the plant involves several steps which may reduce the enzyme activity of the system. Thus, the oxidation rates of amines, which are important in evaluating plant growth-regulating activity, may not provide reliable information.

3.3.6 LIFETIME OF THE SENSOR

The long-term stability of the sensor was tested by calibrating the sensor over a period of 20 days. As shown in figure 16, a considerable decline of the slope was observed for the first 10 days and only a slight variation from 10 to 20 days. Such variations of the slope of calibration graphs are not uncommon for carbon paste modified electrodes, as reported for the determination of catechol using egg-plant tissue (87). Linear calibration graphs even after 20 days indicate the long-term stability of the enzyme system in pea seedlings.

3.4 CONCLUSIONS

The pea seedling-carbon paste sensor has several important advantages over the conventional methods used to monitor the oxidation of plant growth-regulating substances, including low detection limits below micromolar concentrations, fast response and relatively easy construction. Perhaps most interestingly, reliability and good

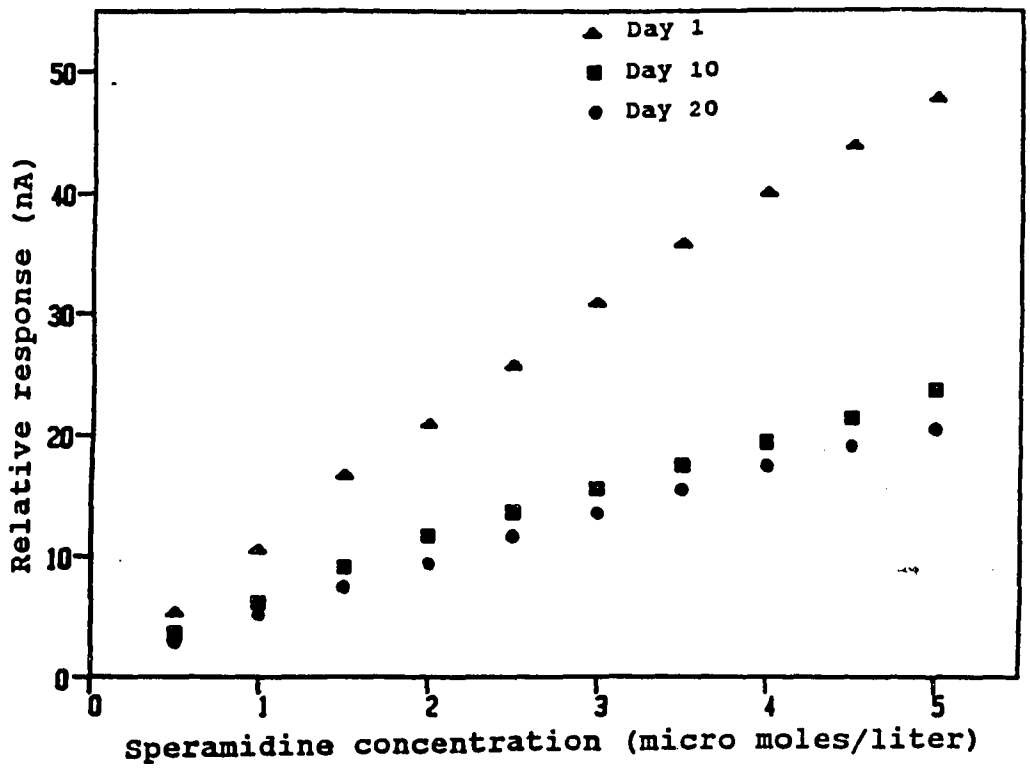

Figure 16. Long-term stability of the mixed carbon paste-pea seedling sensor. ▼, day 1; ■, day 10; ●, day 20.

reproducibility of the data would undoubtedly be useful in evaluating the herbicidal activity of plant growth-regulating substances used earlier (80). Previous methods used for monitoring the oxidation of amines (82,84) involved the addition of a second enzyme, horseradish peroxidase, and these enzymes are not reusable. The carbon paste sensor, on the other hand, can be reused without adding any other enzymes. This type of sensor is also very efficient and convenient in testing newly synthesized herbicides.

CHAPTER 4

CONSTRUCTION AND PROPERTIES OF A PYRAZINAMIDE SELECTIVE BIOSENSOR USING CHEMORECEPTOR STRUCTURES FROM CRAYFISH

4.1 BACKGROUND

4.1.1 CRAYFISH ANTENNULAR PHYSIOLOGY

There is a good deal of analogical ground for the supposition that some peculiar structures, which are evidently of a sensory nature, developed on the under side of the outer branch of the antennule, play the part of an olfactory apparatus.

The antennule (figure 17, A) has a three-jointed stem and two terminal annulated filaments, the outer of which is thicker and longer than the inner, and lies rather above as well as external to the latter.The basal segment of the stem of the antennule is longer than the other two segments put together, and near the anterior end its sternal edge is produced into a single strong spine (figure 17, sp). The stem of the antennule answers to the protopodite of the other limbs, though its division into three joints is unusual; the two terminal annulated filaments represent the endopodite (figure 17, en) and exopodite (figgure 17, ex).

Both the outer (figure 17, ex) and the inner (figure 17, en) branches of the antennule are made up of a number of delicate ring-like segments, which bear fine setae (figure 17, b) of the ordinary character.

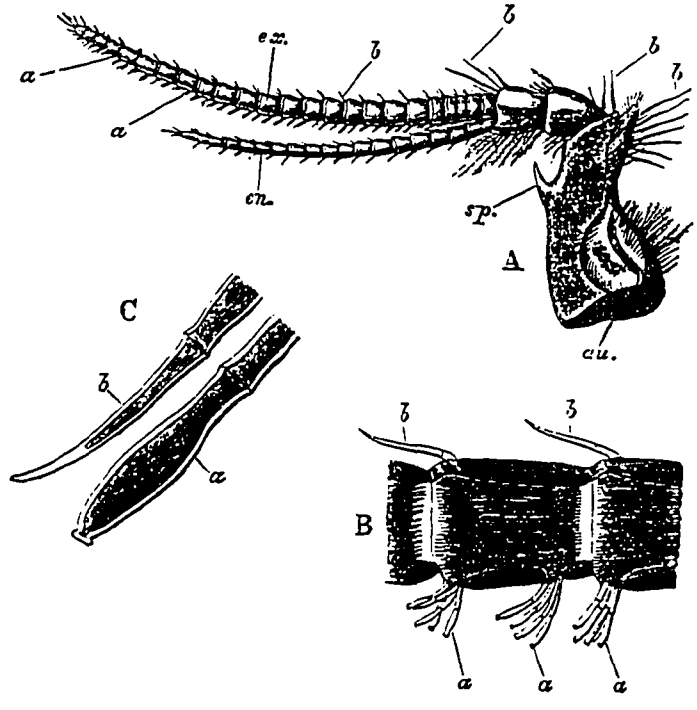

Figure 17. *Astacus fluviatilis.* A, the right antennule seen from the inner side (X5); B, a portion of the exopodite enlarged; C, olfactory appendage of the exopodite; a, front view; b, side view (X300); a, olfactory appendages; au, auditory sac; b, setae; en, endopodite; ex, exopodite; sp, spine of the basal joint (ref 88).

The inner branch, which is the shorter of the two, possesses only these setae; but the under surface of each of the joints of the outer branch , from about the seventh or eighth to the last but one, is provided with two bundles of very curious appendages (figure 17, A,B,C,a), one in front and one behind. These are rather more than 1/200th of an inch long, very delicate, and shaped like a spatula, with a rounded handle and a flattened somewhat curved blade, the end of which is sometimes truncated, sometimes has the form of a prominent papilla. There is a sort of joint between the handle and the blade, such as is found between the basal and the terminal parts of the ordinary setae, with which, in fact, these processes entirely correspond in their essential structure. A soft granular tissue fills the interior of each of these problematical structures, ascribed an olfactory function (88).

4.1.2 NEURONAL BIOSENSORS

Research on neuronal biosensors is greatly facilitated through the introduction of color video microscope technology for the visualization and manipulation of neuronal structures under high magnification as well as the production of permanent visual and data records. As described here, the combination of video imaging with the neurophysiological techniques described earlier (34) substantially improves the reliability and convenience of neuronal biosensor construction while extending the range of experimentation to new sources of chemoreceptor structures.

All of the work reported to date in this field has been based upon the use of various crab species as the source of chemoreceptor structures. Crabs are attractive candidates for neurophysiological research because of their wide availability, extensively studied behavioral correlations, and the relatively easy exposure of their chemoreceptive areas owing to the size of the neuronal structures involved. For analytical purposes, however, crab based neuronal biosensors are severely limited by the need to maintain a specialized electrolytic medium in all solutions (including the analyte) used and because of technical problems of maintaining viable crab neurons in the laboratory.

4.1.3 SINGLE CELL MEASUREMENTS

Recent electrophysiological studies of chemoreceptors located on the walking leg of crayfish revealed that four different pyridine analogs can cause significant stimulation (89). Effectiveness of as a chemostimulant is in decreasing order:

pyrazinamide (K_M=1.5X10^{-6})> 3-acetyl pyridine (K_M=4X10^{-6})> niacinamide (K_M=1X10^{-5})> pyridine-3-aldoxime (K_M=4X10^{-5})

where K_M is the stimulus concentration at which a half maximal response is elicited. Pyrazinamide was the most effective chemostimulant out of 79 pyridine analogs tested. The inferred structural requirements for an optimal stimulatory molecule were that it has a N-containing aromatic ring system with a specific substituent

in the meta position. In our study, chemostimulant potentials of the above four pyridine analogs were tested with the receptor units of crayfish antennule.

4.1.4 PYRAZINAMIDE

Pyridine analogs such as pyarazines occur widely in plants and animal natural products (90,91). Some of these pyrazines have extremely potent aroma and flavoring properties. Behavioral experiments have shown that pyridine or its analogs also act, as stimuli to the human gustatory and olfactory organs, as sexual attractants in the tree shrew, and as marking and alarm substances in various insects (90,92,93). For example, pyrazines such as 2,5 dimethyl-3-isopentyl pyrazine and 2-6-dimethyl-3-pentyl, butyl, and propyl function as powerful releasers of alarm behavior for Odontomachus workers and are probably utilized as defensive compounds (91).

Pyrazinamide (figure 18), an analogue of nicotinamide, is not water soluble and exhibits antimycobacterial bactericidal activity in vitro only in an acid medium, which makes susceptibility studies very difficult. When administered with other agents in therapeutic doses, it may contribute to the total antimycobacterial effect.

Pyrazinamide has been used in the United States primarily for retreatment and only when the disease is a greater threat than the drug's potential toxicity. Sophisticated studies of host metabolism have not explained pyrazinamide's mode of action. This drug is batericidal,

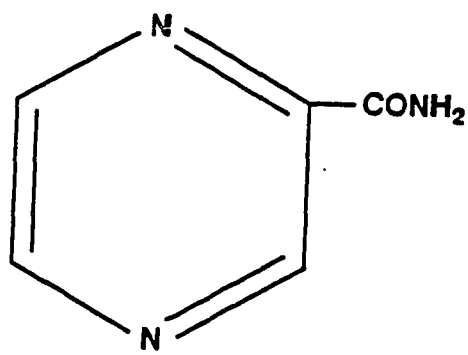

Figure 18. Structure of the antitubercular drug pyrazinamide

especially for intracellular tubercle bacilli, which may explain its efficacy in murine tuberculosis, which is primarily an intracellular disease.

Pyrazinamide is well absorbed orally (time to peak effect is about two hours) and is widely distributed. It is hydrolyzed and hydroxylated to the major excretory product, 5-hydroxypyrazinoic acid, which is eliminated principally by glomerular filtration. Doses exceeding 35 mg/kg (per day) can cause hepatic and liver damage and a number of fatal cases is on record. A convenient and reliable assay procedure for monitoring the mode of action and the dose response behavior of pyrazinamide has not been established. Electrophysiological experimentation described here demonstrates a new approach to develop novel sensors for the determination of such clinically important drugs.

4.1.5 EXTRACELLULAR MICROELECTRODES

The extracellular microelectrodes that are currently in use are of two basic types: (a) micropipettes, filled with an appropriate electrolyte and coupled to the amplifier input stage with a Ag/AgCl or platinum wire; and (b) metal electrodes, electrolytically sharpened to micron tip dimensions and coated except at the tip with glass, varnish, or long-chain polymers that are deposited by vaporization (94).

4.1.5.1 GLASS MICROELECTRODES

The glass micropipette, with a tip diameter on the order of 10-30

micrometer and filled with an electrolyte solution (physiological saline solution), is perhaps the most widely used microelectrode for extracellular recordings. The electrodes are easy to construct and are capable of yielding recordings of comparatively low noise and high quality.

The minimum noise voltage that one would expect to be generated across a glass microelectrode of resistance R will be given by

$$V_{rms}=(4KTR\nabla F)^{1/2}$$

where K is Boltzmann's constant, T is the temperature in degrees Kelvin, and ∇F is the recording bandwidth in Hz (95,96). At room to body temperature

$$V_{rms}\sim(2X10^{-20}R\nabla F)^{1/2}$$

Thus, with a 10 Megaohms electrode and a recording bandpass of 5-10 KHz, one would expect minimum noise levels on the order of 20-40 microvolts rms. It is for this reason that recording microelectrodes should be constructed and filled with solutions of the highest reasonable conductivity, in such a way as to minimize the electrode resistance.

4.1.5.2 METAL MICROELECTRODES

There are three major advantages offered by metal microelectrodes for extracellular, single-unit recording experiments. First, for signals in the spikes frequency range, their impedance may be only 0.1-0.5X that

of a glass microelectrode with equivalent unit-isolation properties. Thus, for this frequency range of signals, a metal microelectrode may offer superior (lower) noise characteristics. Second, when constructed of stainless steel, tungsten, or iridium, the electrode will have sufficient mechanical rigidity for puncturing cellular structures. Finally, metal microelectrodes of desirable tip shape and size may be prepared in large quantities with comparable ease.

4.1.5.3 CARBON-FIBER MICROELECTRODES

Another technique for fabricating extracellular microelectrodes is to use a 7-10 micrometer carbon fiber that has been encased in a glass micropipette for strength (97). These microelectrodes appear to have recording qualities similar to those of tungsten microelectrodes (98) and are easier to construct (99). The carbon-fiber electrode can be silver-plated to reduce the impedance and noise.

4.1.5.4 PRINTED CIRCUIT ELECTRODES

The most elaborate extracellular microelectrodes are those made with printed-circuit technology (100,101). The advantage of this technology is that large quantities of the electrodes can be fabricated with very precise dimensions. The disadvantage of printed-circuit electrodes is the need for specialized fabrication equipment that usually is not available to most physiology laboratories.

4.1.6 GRASS MODEL P-15 MICROELECTRODE PREAMPLIFIER

The P-15 is a solid-state, battery powered, differential AC preamplifier designed to record a wide range of bioelectric phenomenon including recording of Electroencephalogram, Electrokardiogram etc. The high input impedance, capacity compensation, low noise and fast rise time characteristics of P-15 is ideal for dependable recording of nerve, muscle action potentials or intracellular recording. The variable bandpass filters, with lower settings of 0.1-300 Hz, and high cutoffs of 0.01-50 KHz (1/2 amplitude frequencies) allow the recording bandpass to be restricted to the range of frequency components in the biological signal, with an attendant decrease in unwanted noise frequencies. Input resistance of P-15 is 200 megohms differential and the noise level of 20 microvolts (peak to peak) is typical.

4.2 EXPERIMENTAL

4.2.1 REAGENTS

The pyridine analogs, pyrazinamide, niacinamide, 3-acetyl pyridine and pyridine-2-aldoxime and other possible stimulants such as adenosine monophosphate, taurine, kainic acid, glutamic acid, norephinephirine, betaine, taurocholic acid, glutamic acid, gama amino butaric acid, cis 8-dodecylacetate, menthol, butanol, sucrose, and nicotinamide adenine dinucleotide were purchased from Sigma Chemical Company. All stock solutions and serially diluted solutions for certain stimulants were prepared in tap water and stored at 40^0F. The

neuro-bathing solution was prepared in deionized water and had the following composition (mmol/l): Na^{+} 205, K^{+} 5.4, Ca^{+2} 13.5, Mg^{+2} 2.6, Tris malate buffer 10; pH 7.6.

4.2.2 CRAYFISH ANTENNULES

The crayfish (*Procambarus clarkii*) (figure 19) were obtained from the Manoa stream near the campus and maintained in a fresh water tank for later use. An anatomical diagram of a crayfish is shown in figure 20 (102). In this study, an antennular section of the crayfish was used as the chemosensitive unit. Each crayfish has four antennules which could be used effectively for different experiments. Figure 21 shows a close-up view of the distal end of a crayfish antennule as seen under the phase contrast microscope (150X). The actual length of an antennule can vary with the age of the species and is in the order of 1-2 cm. Different types of receptors such as chemo-sensory receptors, mechano-receptors, and pressure or temperature receptors are located in the aesthetascs (the fine hair-like structures) of the antennules. The individual aesthetascs are micrometer size and require special equipment for visualization and manipulation. Figure 22 shows a single aesthetasc, under high magnification, photographed from the video screen of the microscope monitoring system. The delicate structure represents the ultimate size limit and goal for chemoreceptor structure based sensors.

Figure 19. *Procambarus clarkii*

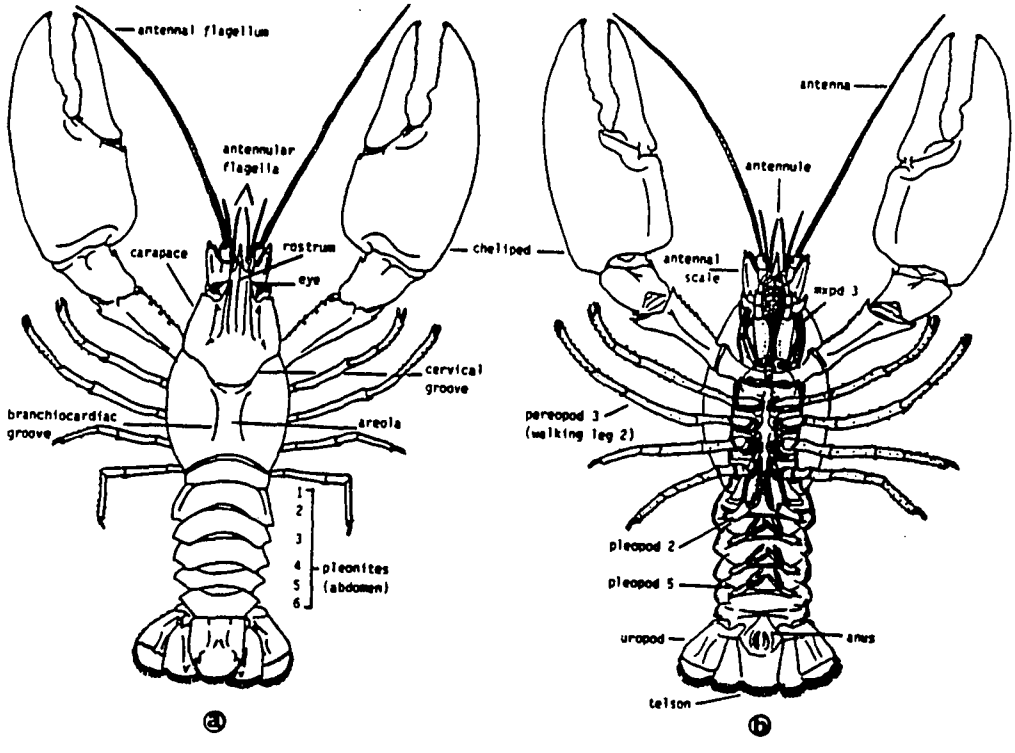

Figure 20. Dorsal (a) and ventral (b) view of a crayfish showing anatomical features.

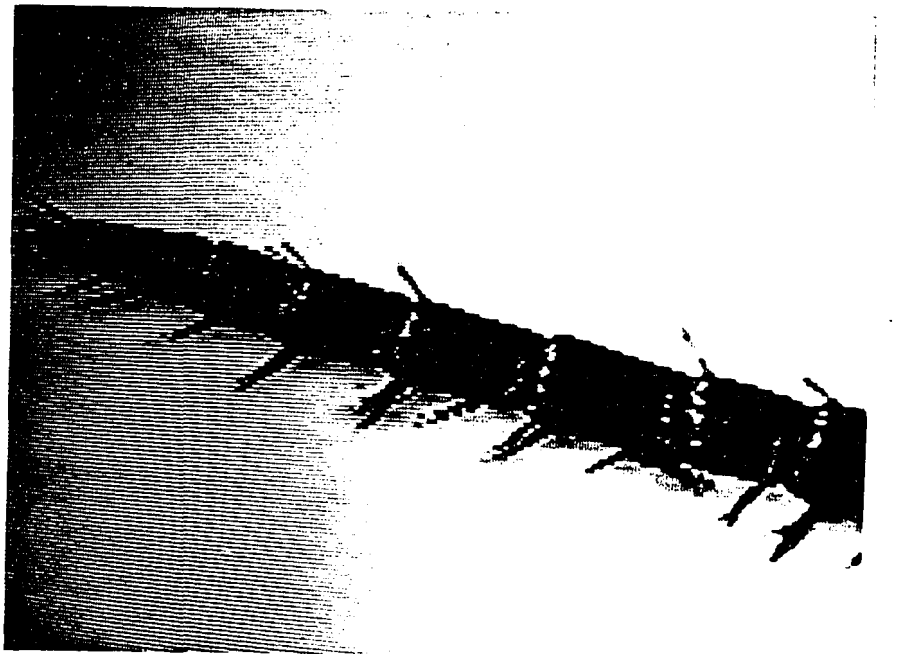

Figure 21. Video image of the distal end of a crayfish antennule (magnification 150X).

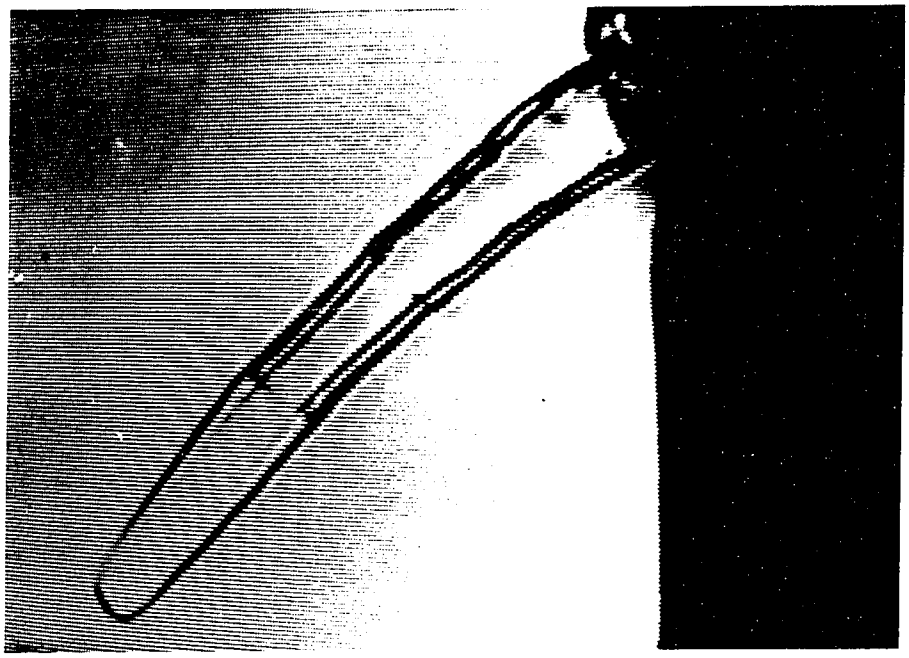

Figure 22. Fine structure of an individual aesthetasc under high magnification (1700X).

4.2.3 APPARATUS

A schematic diagram of the apparatus used for this experimentation is shown in figure 23. The plexiglass cell was designed to hold the antennules in place on the mechanical stage of the Bio-star trinocular dissecting microscope. The cell mainly consists of a circular chamber attached to a carrier stream line. The neurobathing chamber (circular bath) and the carrier stream-line were connected to each other by a small hole. Thus, crayfish antennules can be mounted in such a way that the nerve fibers are exposed to the neurobathing solution and the chemosensitive portions to the fresh water carrier-stream for testing possible stimulants. Reference and ground wires were inserted into the neurobathing chamber.

A glass micropipette containing a Ag/AgCl element was also positioned in this chamber, with a micromanipulator, to measure the action potentials of different nerve cells. A small amount of neurobathing solution was drawn into the micropipette with a suction syringe in order to create a conducting medium between the Ag/AgCl element and the nerve cells. Once a good seal was made between the tip of the micropipette and the nerve cells, action potentials can be recorded. A solution carrier stream was pumped through the plexiglass cell using a Rabit-Plus digital peristaltic pump. A four-port, two-way valve with a sample injection loop was used to apply a constant concentration of stimulus solution to the chemoreceptors for a period of 30 seconds. The indicator electrode potential with respect to ground

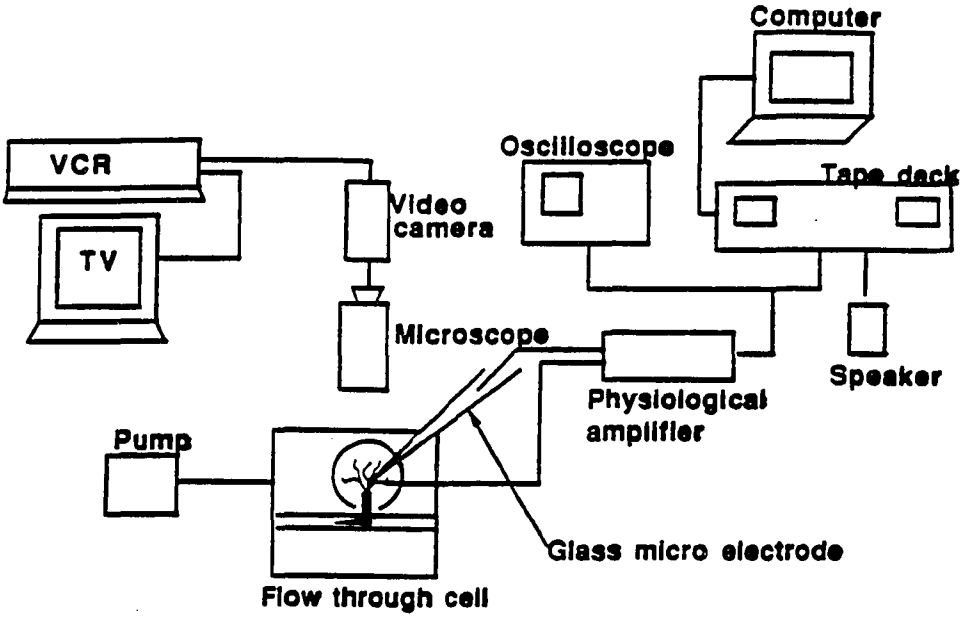

Figure 23. Schematic diagram of the experimental set up.

and reference was amplified 10, 100, or 1000 times, as appropriate, using a Grass Instruments neurophysiological preamplifier. Output of the amplifier was monitored on Tekronix 564B storage oscilloscope and also stored on an audio tape using a TEAC v-385 stereo cassette recorder. A microphone enabled an oral account of the experiments to be stored in one channel of the stereo tape while the data were stored on the other channel. Action potential data analysis were done using an IBM model (c) DTK 386 BIOS Ver 4.25 personal computer.

The Bio-star model 1820 inverted biological microscope used for this experiment was capable of magnifying the objects in a range from 40X to 450X. Use of phase contrast unit was particularly significant to clearly visualize the depth of the antennule and the aesthetascs. The video unit coupled to the microscope system consisted of a video camera, a color monitor and a video recorder. A Hitachi vk-c150 color camera featuring 340 lines horizontal resolution, 15.734 Khz and 59.94 Khz horizontal and vertical scanning frequency respectively, 46 dB signal/noise ratio, and 3.579545 color carrier frequency is mounted to the trinocular tube of the microscope. Signal output of the video camera was displayed on the Sony color video monitor (model PVM-1380) with a resolving power of 250 TV lines. The video unit attached to the microscope produced highly magnified images ranging from 150X to 1700X. All video images were stored on a video tape, using a JVC video cassette recorder (model HR-D660U), for later use. Color pictures of the fine structure of an antennule were obtained by photographing the video

screen using a 35 mm camera (CHINON CM-5).

4.2.4 PROCEDURE

Upon dissecting the upper part of the antennules (2-3 mm), nerve fibers can be visualized through the microscope. The dissected antennule was carefully mounted on the flow-through cell so that a considerable length of the bottom part of the antennule, which contains chemosensory hairs (aesthetascs) remains in the carrier stream and the exposed nerve fibers are placed in the circular chamber. Neurobathing solution was added immediately; tap water was also pumped continuously as a carrier stream to prevent possible damage to the exposed nerve cells and the rest of the antennule from dehydration. Ground and reference wire electrodes were connected to the physiological amplifier. The tip of the micropipette electrode was positioned on the exposed nerve fibers until action potential spikes were observed and heard on the audio speaker. The video monitoring system is particularly helpful in viewing the contact position and positioning the contact electrode as shown in figure 24. Once a significant action potential is observed, various stimulant can be injected into the carrier stream using the sample injection valve. Volume of the sample loop was .25 milliliters. Serially diluted analytes were injected for analytes which showed significant stimulation to construct dose/response curves. The frequency of baseline action potentials (no stimulant in the carrier stream) was also recorded and

Figure 24. A video image of the nerve fiber with the glass capillary electrode in place (magnification 750X).

subtracted as a "blank" from the signals produced by the chemostimulants. Segments of action potentials corresponding to background response and stimulant response at the maximum were selected and digitized at a rate of 50 KHZ for 5.12 seconds using the "einsight" chemometrix data analysis program. Frequency of firing was calculated from the histogram plots which show the number of potential spikes that fall into different amplitude ranges (in mV). Actual frequency response (stimulant response - background) was plotted against the stimulant or log stimulant concentration where appropriate to obtain dose/response plots. Selectivity of the sensor was tested by injecting some structurally related compounds and also other possible stimulants such as essential amino acids, excitatory amino acids, neurotransmitters, agonists, and antagonists. Lifetime of the sensor was also studied by injecting primary stimulant (1 mM pyrazinamide) at one hour intervals until no response could be seen.

4.3 RESULTS AND DISCUSSION

The sensory system of the crayfish is provided with a large number of setae. Which of these are chemo-sensory, mechano-receptors, pressure, or temperature receptors, remains problematical. In some instances, chemoreceptors are closely associated with the mechano-receptors that cause tactile responses. Food detection of crayfish is largely a function of the specialized setae and aesthetascs located in the under side of the outer flagellum of the antennule

(103,104). Chemoreceptors are located in other parts of the crayfish such as antennae, chelae and dactyl of the first and second walking legs and certain mouth parts (,103,105).

The molecular recognition units involved in the construction of intact chemoreceptor based sensors are extremely small and can only be visualized using a high power (magnification) microscope. Yet, manipulation has to be done by viewing such small units through the eye pieces of a microscope. This method is not convenient (in some cases impossible) when the fine structure of receptors cannot be visualized clearly. This difficulty was significantly eliminated by using the modern video image technology described here. Video camera/monitor unit attached to the microscope produced excellent color pictures of fine structures while magnifying the objects beyond the limitation of the microscope. As seen here, total magnification up to 1700X could be achieved using the video unit compared to the 450X highest possible magnification obtained using the microscope itself.

Higher magnification is essential in constructing neuronal biosensors using fine structures of various species. Figure 22 illustrates the video image of an aesthetasc (1700X) on the crayfish antennule. Typical length and diameter of the aesthetasc was 102 and 12 micrometer, respectively, as measured from the video image. As described earlier, different types of receptors are located on the nerve cells inside these aesthetascs. Binding molecules can penetrate into the receptor cells and cause depolarization of potential gradients across

the cells. Equilibrium is re-established very quickly after returning to the resting potential. Potential spikes are generated from this rapid ion channel equilibrium process and the signal is propagated along the nerve cells to the brain. In early work, such action potentials were recorded from a remote end of the nerve fibers using a glass capillary electrode (figure 24). The optimal contact position of the electrode with the nerve cells needs to be determined in order to obtain selective responses from different stimulants; this process is greatly facilitated using the manipulation/video imaging techniques described here and permits a more systematic approach to receptor identification.

The use of neuronal structures from fresh water crayfish in biosensor construction demonstrated their satisfactory analytical behavior in ordinary tap water (or distilled water). The use of crayfish significantly reduces the interference effects introduced by the need for sea water matrices and simplifies the experimental protocol. In nature, sea water crabs are very sensitive to external variations such as temperature and salinity changes in their environment. Thus, sensors made using antennular sections of crabs also show the same behavior. In some instances, these sensors provide false positive results irrespective of the analyte tested because of such external variations. Since crayfish are fresh water species, tap water or de-ionized water could be used effectively for both carrier stream and analyte media for the development of crayfish neuronal sensors. Chemoresponse data obtained from these sensors provide more reliable informations owing

to lesser interferences from the background. Excellent thermal stability of crayfish receptors also provides some advantages. Temperature differences between the analyte and the carrier solution have no significant effect on the action potential measurements. As reported earlier (106), activity of amino acid sensitive receptors in the crayfish walking leg was not affected within a broader temperature range from 0^0C to 26^0C. Thus, action potential measurements were carried out at the room temperature (22^0C) without special temperature control of the flowthrough cell.

The use of crayfish neuronal structures in biosensor construction offers an extension of analytical capabilities to compounds not previously measured. The sensitive measurements of the important antitubercular drug pyrazinamide with high selectivity over structurally related compounds are clinically important. Pyrazinamide represents a potential chemostimulant for the receptors in crayfish antennules as revealed during the screening test of the sensor with structurally related pyridine analogs and other reported chemostimulants. Repeated chemoresponses from several crayfish antennules confirmed the presence of receptor cells sensitive to pyrazinamide.

4.3.1 MULTI UNIT DOSE/RESPONSE

The dose/response curve obtained from serially diluted pyrazinamide solutions is shown in figure 25. This particular data set corresponds to

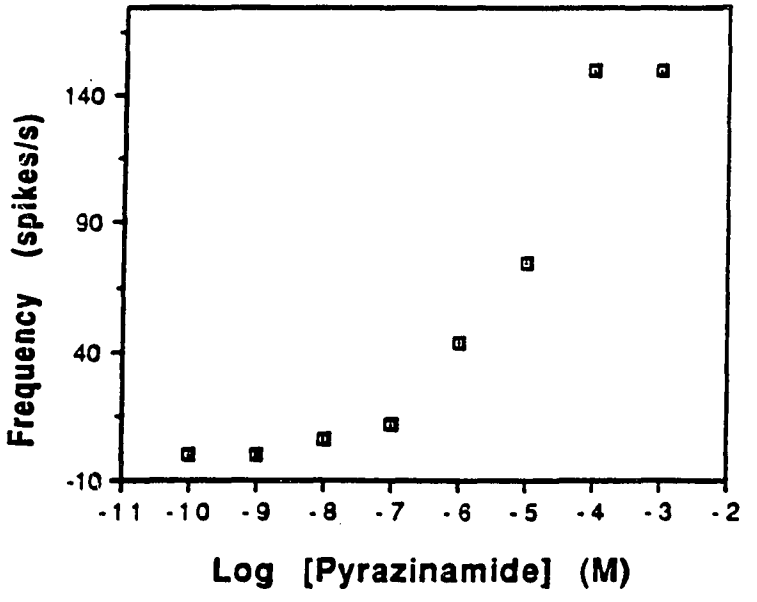

Figure 25. A multi-unit dose/response curve of the sensor to pyrazinamide.

multi unit action potential responses. Multi-unit data consists of potential spikes of varying amplitude. Extracting the individual units responding to a chemostimulant is rather complicated owing to the complex nature of the response pattern. In some instances, multi unit responses can be seen when chemoreceptors are closely associated with the mechano receptors causing both tactile and chemoresponses. Two or more action potential units having different amplitudes may also respond to a particular stimulant simultaneously, creating such multi unit response patterns. Window discriminators have been used earlier to distinguish and selectively identify action potential spikes obtained from various chemostimulants. As reported earlier (107), this method was reliable only for the analysis of single unit response data. In this study, multi unit responses were analyzed using a chemometric data analysis program. Histogram plots showing the number of potential spikes falling into different amplitude ranges (mV) were obtained for each of the serially diluted analytes. Response frequency in each bin of the histogram plots were compared to extract the best data set which shows a linear relationship with the analyte concentration. Detailed description of the data analysis techniques is reported elsewhere (108). A broader concentration range of the stimulant was initially used to determine the dose/response behavior. Figure 25 indicates an increase in response from 10^{-7} to 10^{-4} M analyte concentration. No change in frequency response above 10^{-4} M pyrazinamide may be due to the saturation of receptors causing adaptation. Frequency response shows a

linear relationship with the concentration of pyrazinamide from 10^{-5}M to 10^{-4}M. This was investigated further by injecting serially diluted pyrazinamide solutions within a narrow concentration range.

4.3.2 SINGLE UNIT RESPONSE PATTERNS

Single unit response of the sensor to $3X10^{-5}$M pyrazinamide, as monitored on the oscilloscope, is shown in figure 26 along with the background activity (figure 27). Actual potential responses were amplified by a factor of 1000 using a low noise differential A.C. preamplifier. Increased frequency of potential spikes is a clear indication of chemostimulation by pyrazinamide. The approximately equal magnitude of the potential spikes indicates a typical single unit response pattern and the time scale of these plots also shows the response time of the sensor to be of the order of a few milliseconds. As reported previously, such short response times are typical for intact chemoreceptor based sensors (40,41,42,107) owing to rapid ion transport upon substrate binding to the receptor site. Acetylcholine receptors have been used extensively as a model to explain the ion channel opening mechanism.

4.3.3 SINGLE UNIT DOSE/RESPONSE

Figure 28 represents a single unit dose response curve obtained with pyrazinamide. Single unit response data are easy to analyze and also very reliable in terms of quantitative measurements. Since the

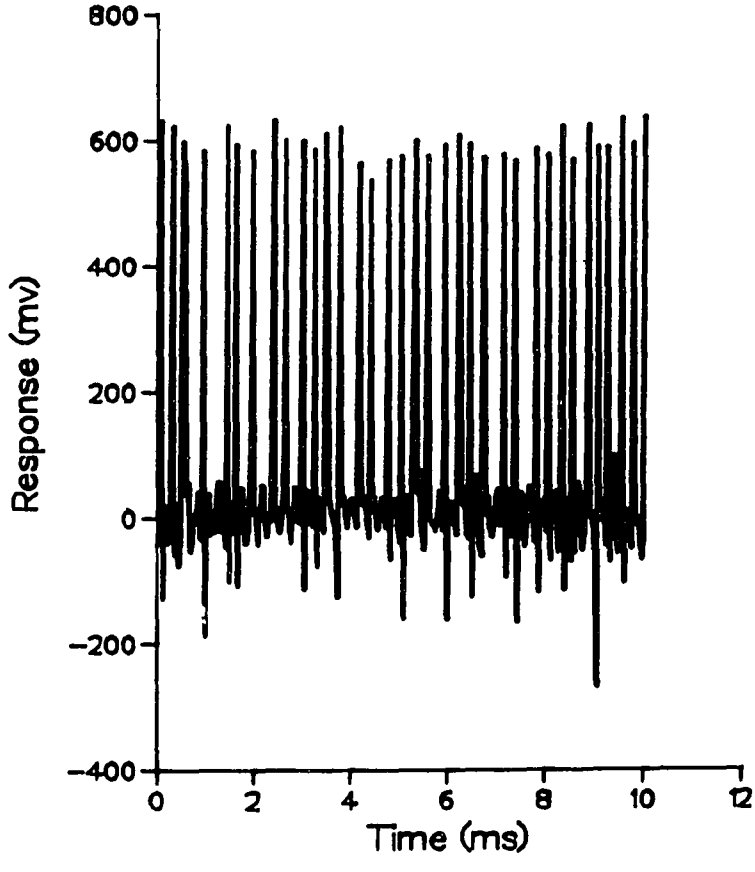

Figure 26. Record of single unit response of the sensor to $3X10^{-5}$ M pyrazinamide.

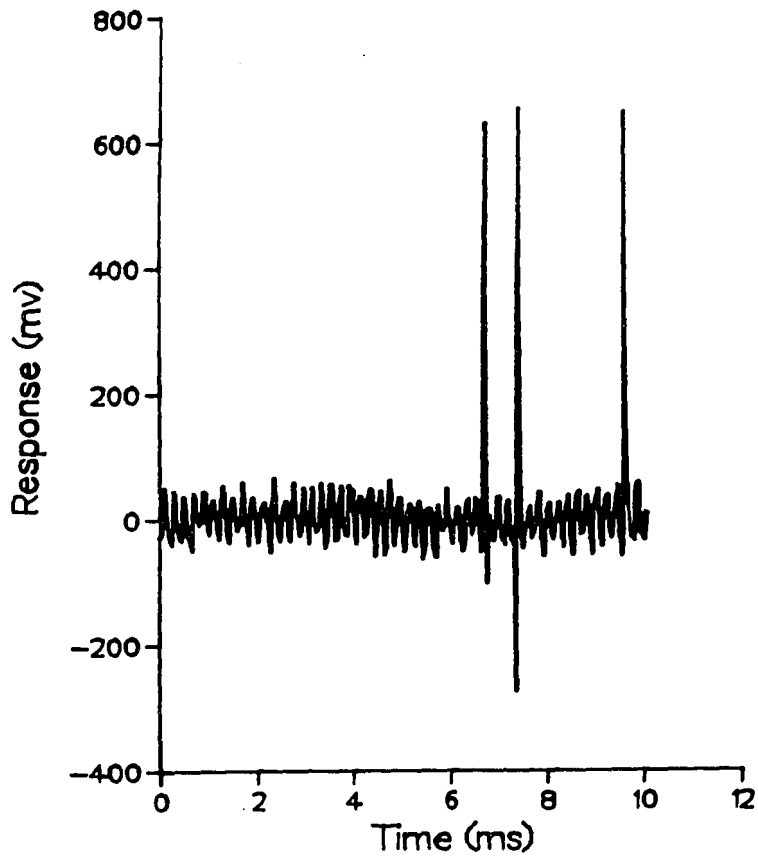

Figure 27. Background response of the sensor prior to the injection of analyte.

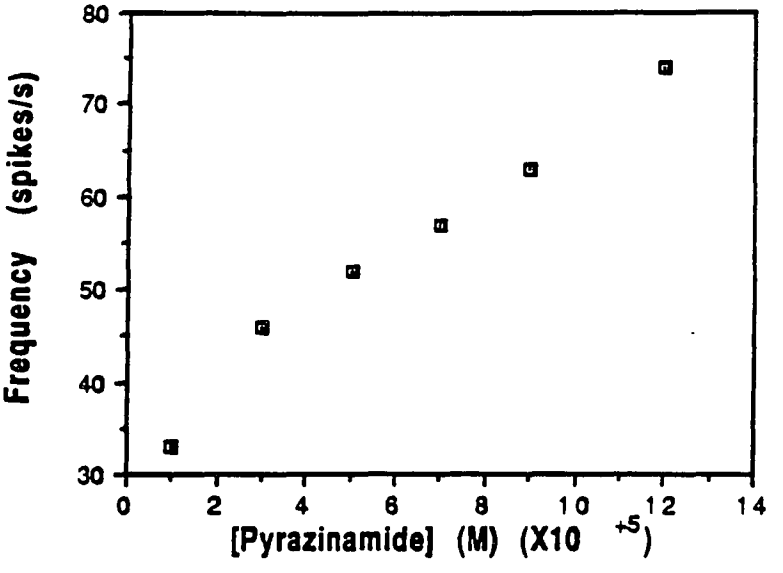

Figure 28. Single unit dose/response curve of the sensor to pyrazinamide.

magnitudes of the potential spikes are almost the same, frequency of firing can be easily calculated. In this case, only one bin of the histogram plots indicates the response frequency due to the potential spikes of same amplitude. The slope of the dose/response curve indicates a linear relationship with the analyte concentration; such a linear range is useful for determining an unknown concentration of the analyte. Recent experiments with single unit data from several crayfish antennules produced almost identical maximum frequency responses (spikes/sec.), demonstrating good reproducibility of the neuronal sensor. The maximum frequency of 42 ± 1 (spikes/sec.) was obtained with 3 antennules from different crayfish for 1 mM concentrations of analyte.

4.3.4 SELECTIVITY MEASUREMENTS

One remarkable feature of intact chemoreceptor based sensors is their high degree of selectivity. Such selectivity is also demonstrated in this study. Over 15 different analytes including essential amino acids, neurotransmitters, hormones, alcohols, sugars, agonists, antagonists and structurally related compounds were tested as possible stimulants along with the primary stimulant pyrazinamide. Only the primary analyte yielded a response, indicating the unique binding properties of the chemoreceptors.

4.3.5 LIFETIME

The lifetime of the crayfish sensors was much better than those of corresponding crab antennular based sensors. Typical lifetimes were of the order of 8-10 hours depending on the concentration of the analyte injected. In some instances, injection of highly concentrated analyte (>1 mM) diminished the response within 2-3 hours, perhaps because of nerve cell damage. Excised antennule can be kept viable for more than two days in saline media at 15^0C. Extension of lifetimes is a critical factor in the effort to develop reusable sensors.

CHAPTER 5

REUSABLE NEURONAL BIOSENSOR FOR THE DETERMINATION OF 3-ACETYL PYRIDINE

5.1 BACKGROUND

Crayfish antennular based sensors offered several advantages over corresponding crab sensors in terms of less interferences and better lifetimes (109). To date, however, relatively little attention has been focused on the reproducibility, reusability and lifetime of the neuronal biosensor system (41). The construction and characterization of a reusable neuronal biosensor selective for a clinically important neurotoxin, 3-acetyl pyridine is reported with emphasis on current status of the lifetime extension studies of neuronal sensors.

5.1.1 3-ACETYL PYRIDINE

The introduction of chemical lesioning methods that employ toxic agents such as 6-hydroxydopamine and kainic acid has represented a significant advance in the experimental investigation of central nerve system organization. The search for lesion inducing substances has revealed that certain vitamin analogs may also induce specific centers selectivity. One such agent is the nicotinamide antagonist, 3-acetyl pyridine (figure 29), the toxic effects of which are the results of competition between it and nicotinamide for incorporation into NAD. The pathological changes induced by this substance are thus a reflection of

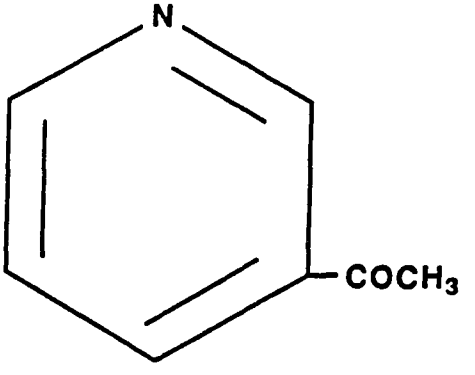

Figure 29. Structure of the neurotoxin 3-acetyl pyridine.

the inhibition of the nicotinamide-dependent metabolic pathways (110). 3-Acetyl pyridine has been known for 20 years to induce degeneration of inferior olivary neurons, followed by the loss of the climbing fiber input to the cerebellum (110,111,112).

Most recently, 3-acetyl pyridine has been used as a starting material for the preparation of 9-substituted 6H-pyrido [4,3-b] carbazoles, which are useful as schistosomicides and antitumor agents (113).

This is the first report of a biosensor selective for the neurotoxin 3-acetyl pyridine and may represent a contribution to the area of clinical chemistry. Characterization of the novel sensor in terms of selectivity, reproducibility, reusability, lifetime, and dose/response relationship is reported.

5.1.2 WINDOW DISCRIMINATOR

The simplest method of separating single-unit spike trains is with the use of a simple "window discriminator" (figure 30). In such a device, the input signal is fed to two voltage comparators, whose reference inputs define the upper and lower limits of a "voltage window". Subsequent circuitry is arranged so that the device generates an output pulse only if a voltage signal that exceeds the lower limit of the window does not (within a following finite time period) also exceed the upper limit. By having several such windows, whose upper and lower limits are adjustable, it is possible to separate the spike trains of several simultaneously recorded units.

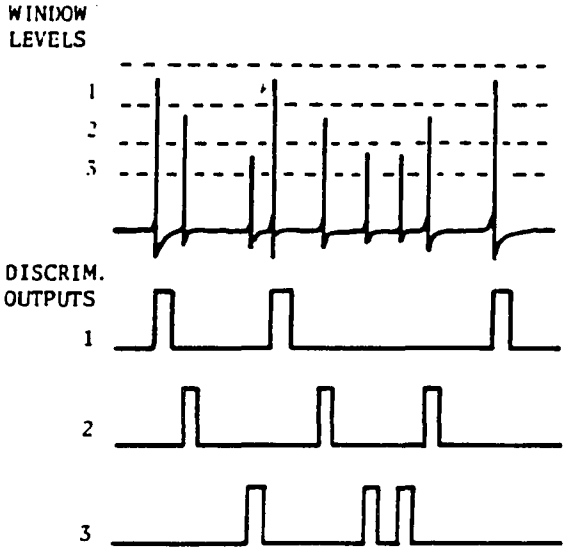

Figure 30. Typical window discriminator output.

5.2 EXPERIMENTAL

5.2.1 REAGENTS

All reagents were of analytical grade and solutions made up with distilled or tap water and stored at 40^0F.The neurotoxin 3-AP and other possible stimulants (not listed in page 75) such as pyruvic acid, fructose, phenol, horseradish peroxidase, insulin, 5-5 diphenylhydantain and dopamine were purchased from Sigma Chemical Company. The nerve bathing solution was prepared according to the procedure described previously (page 76).

5.2.2 APPARATUS

A detailed description of the experimental apparatus is given in chapter 4 (page 81-83). Action potential data were analyzed by using a Newwark Electronic digital event counter and Coulbourn window discriminator, instead of "einsight" chemometrix data analysis program, in order to obtain frequency response values (spikes/sec.). Cricket graph 1.2 version was used to plot the frequency response data on a Macintosh computer.

5.2.3 PROCEDURE

Preparation and the recording techniques of the crayfish antennular based sensor are similar to the procedure described in chapter 4 (page 84-86). Action potential responses were obtained for replicate injections of the primary stimulant at 1 mM and 0.5 mM concentrations.

The system was flushed with tap water or de-ionized water for five minutes between each stimulant addition to minimize any adaptation. Serially diluted primary stimulant solutions were also injected into the carrier stream in order of increasing concentrations. Selectivity of the sensor was tested by injecting more than 15 possible stimulants along with the primary stimulant. Lifetime of the excised antennule was monitored over a period of one week. Antennules were kept in saline solution saturated with oxygen at 12^0C during lifetime studies.

The action potential sequence was divided into 8 sec. time intervals (e.g. interval 1 from t=0 to t=8 sec., interval 2 from t=8 to t=16 sec. etc. assuming t=0 as the beginning of stimulation) and the number of spikes in each time interval was divided by 8 sec. to calculate the frequency response. Maximum spike frequencies corresponding to replicate injections of the primary stimulant were plotted against trial number to study reusability of the sensor. Dose/response relationships were obtained by plotting the maximum response frequencies, which correspond to stimulation from serially diluted analyte, against the stimulant concentration.

5.3 RESULTS AND DISCUSSION

5.3.1 DELAYED RESPONSE

Previously, a train of spikes was seen immediately after the stimulant reached the antennule (40,107). This was not observed with 3-acetyl pyridine as the stimulant. Instead, a delayed response was

observed, with the latency period remaining constant for a given antennule. Perhaps, long diffusion path ways of stimulant molecules to the receptor sites can cause such delayed response patterns. The exposed time of the antennule to the stimulant was 30 seconds for each 0.25 ml injection. Thus, a latency period of over 30 seconds indicates that the actual concentration of stimulant sensed by the antennule is much lower than the injected analyte concentration since no stimulant is in the vicinity of the antennule. Latency periods of approximately 12, 45, 53, and 57 seconds were seen with four different antennules.

5.3.2 REPRODUCIBILITY

Figure 31 shows typical frequency response curves obtained from 9 replicate injections of 1 mM 3-acetyl pyridine. All the curves indicate maximum responses during the third time interval (i.e. frequency response between t=16 and 24 s., assuming t=0 as the beginning of stimulation). The mean value of frequency responses within each time interval in figure 31 was plotted against the interval no. as shown in figure 32. Error bars indicate the standard deviation of mean frequency response values. Significantly high coefficient of variation (over 50%) for the data points in figure 32 indicate the poor reproducibility of the sensor at 1 mM level of 3-acetyl pyridine. Perhaps, at these high concentrations of analyte, activity of the nerve cells could be diminished due to possible toxic effects. Replicate injections of such high concentrations of analyte can further damage the receptor cells

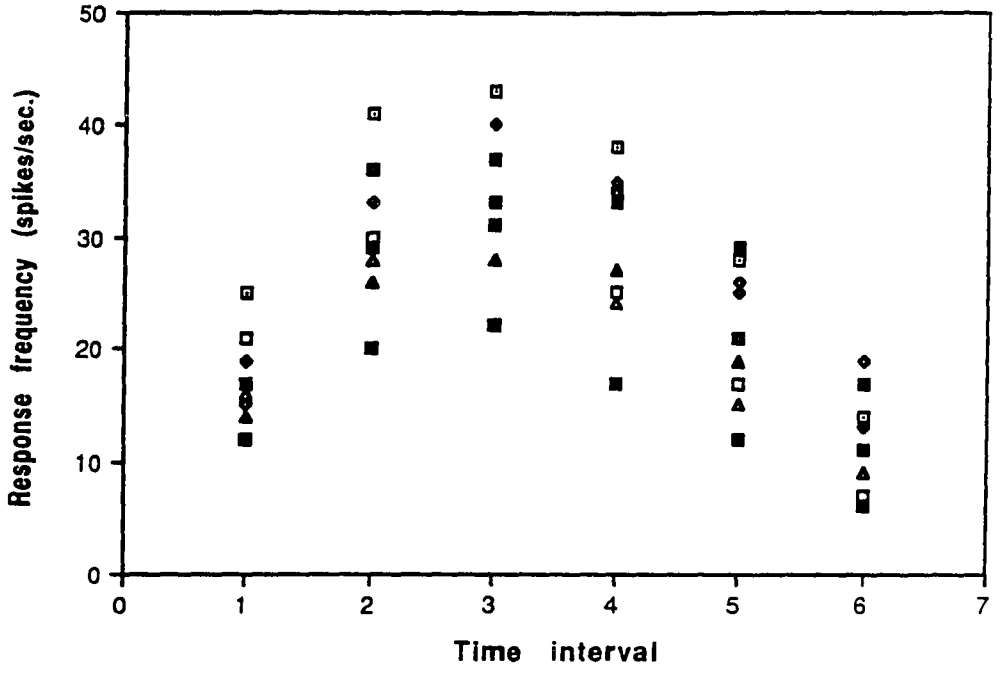

Figure 31. Frequency response curves from 9 replicate injections of 1 mM 3-acetyl pyridine.

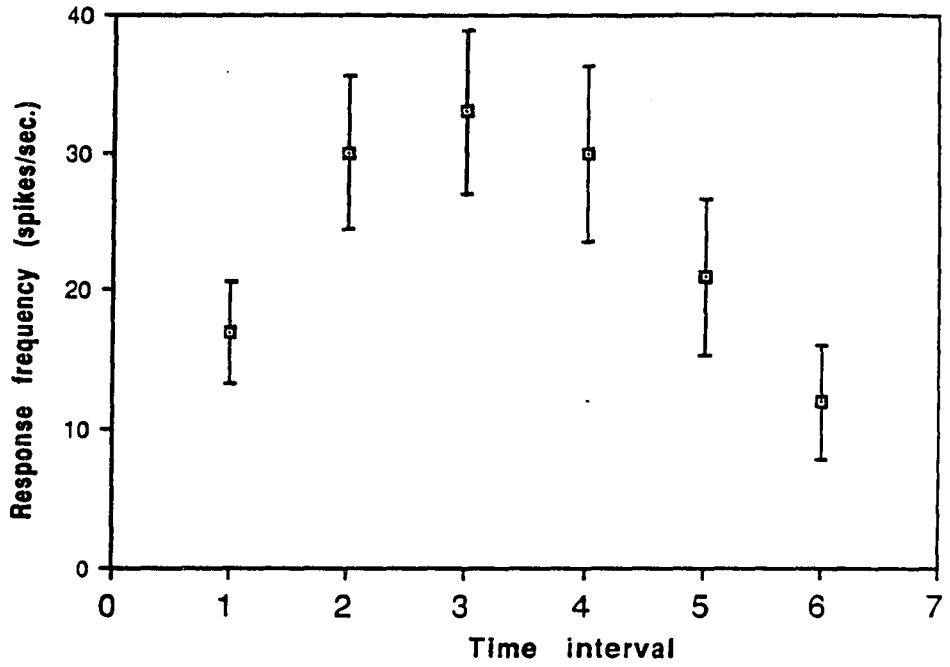

Figure 32. Mean frequency response curve at 1 mM 3-acetyl pyridine.

because of continuous exposure. Although the saturation of receptor sites with the stimulant may also have some effect on the response, adequate time was allowed between two injections to prevent any adaptation. Substrate/receptor binding processes are in general, reversible and the tendency to saturate receptor sites is almost negligible. The influence of stimulant concentration on the reproducibility of the action potential data was investigated further. Figure 33 shows the mean frequency response curve obtained from 9 replicate injections of 3-acetyl pyridine at 0.5 mM concentration. The significantly reduced standard deviation (coefficient of variation of 10% or less) of data points indicates the good reproducibility of the sensor at a lower concentration of the stimulant. Perhaps any toxic effects from 3-acetyl pyridine to the nerve cells were greatly reduced in more dilute solutions, thus providing more reproducible neuronal activities.

5.3.3 REUSABILITY

Unlike other electrochemical sensors, no research thus far has been conducted on the reusability of neuronal sensors. This was reported, for the first time, using the crayfish antennular based sensor. Maximum frequency responses from replicate injections of 1 mM stimulant were plotted against the trial number, as shown in figure 34. The considerable reduction of the response frequencies (over 50%) once again indicates poor reusability of the sensor at high concentration.

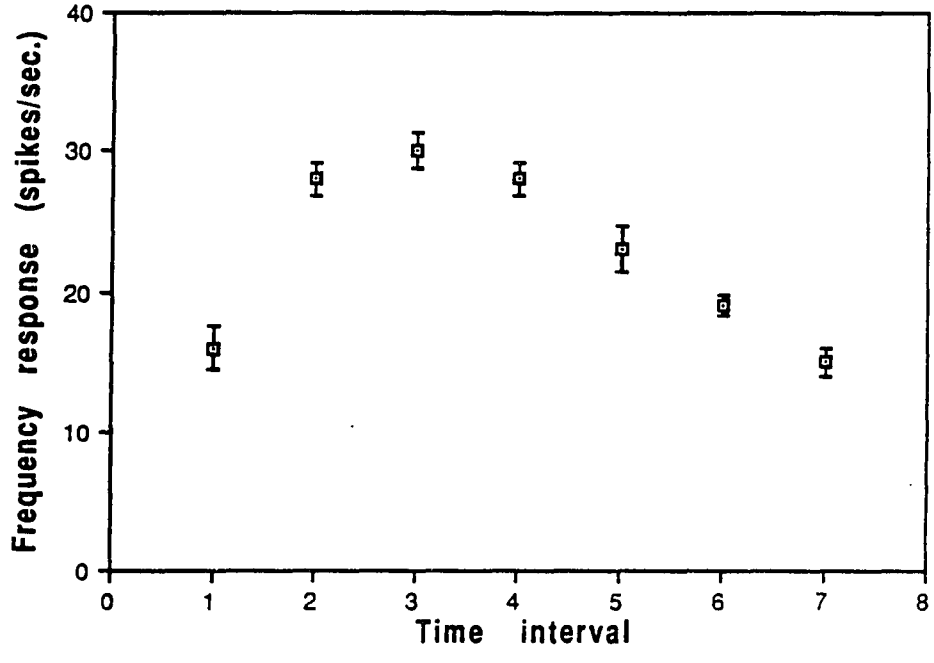

Figure 33. Mean frequency response curve at 0.5 mM 3-acetyl pyridine.

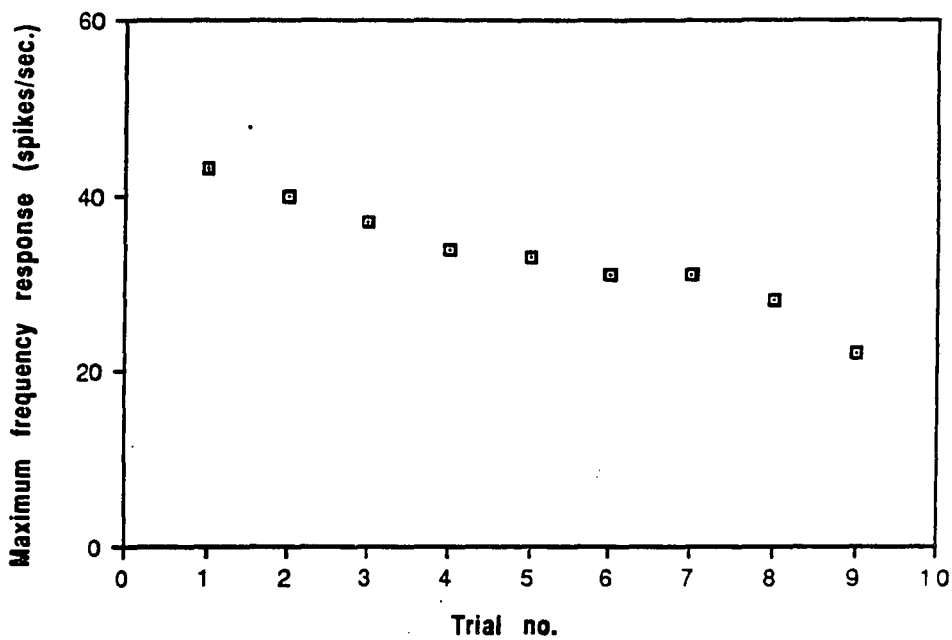

Figure 34. Reusability of the sensor at 1 mM 3-acetyl pyridine.

Figure 35 clearly shows that at a lower concentration (0.5 mM) an almost identical response (coefficient of variation of less than 10%) can be obtained from replicate injections of the primary stimulant. This result indicates the feasibility of developing reusable neuronal biosensors in the future. As seen here, the concentration of stimulant has a significant bearing on the reusability of neuronal sensors.

5.3.4 SINGLE UNIT DOSE/RESPONSE RELATIONSHIP

Figure 36 represents a single unit dose response curve obtained with serially diluted 3-acetyl pyridine. A quite broad concentration range of the stimulant was initially used to determine the dose/response behavior. Figure 36 shows an analytical proportionality between maximum frequency and stimulant concentration over three orders of magnitude in concentration. Figure 37 shows a single unit dose/response curve obtained for a one order of magnitude change in stimulant concentration. The intercept of the regression line gives a high frequency response even at zero concentration of stimulant. This is because the selected concentration range is quite close to the plateau of the saturation curve which was obtained from single cell measurements, as reported previously (89). The pH of the carrier stream and the analyte solution was almost the same (7.5), regardless of the concentration of analyte solutions, thus eliminating any pH effects on the response of the sensor. The time scale of the frequency response was in the order of milliseconds, indicating the extremely short

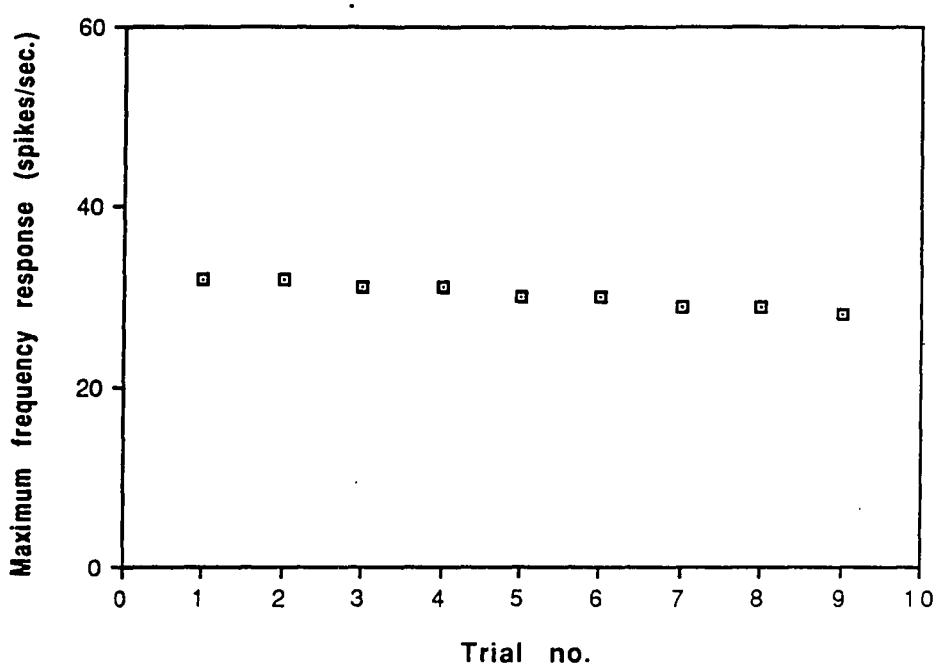

Figure 35. Reusability of the sensor at 0.5 mM 3-acetyl pyridine.

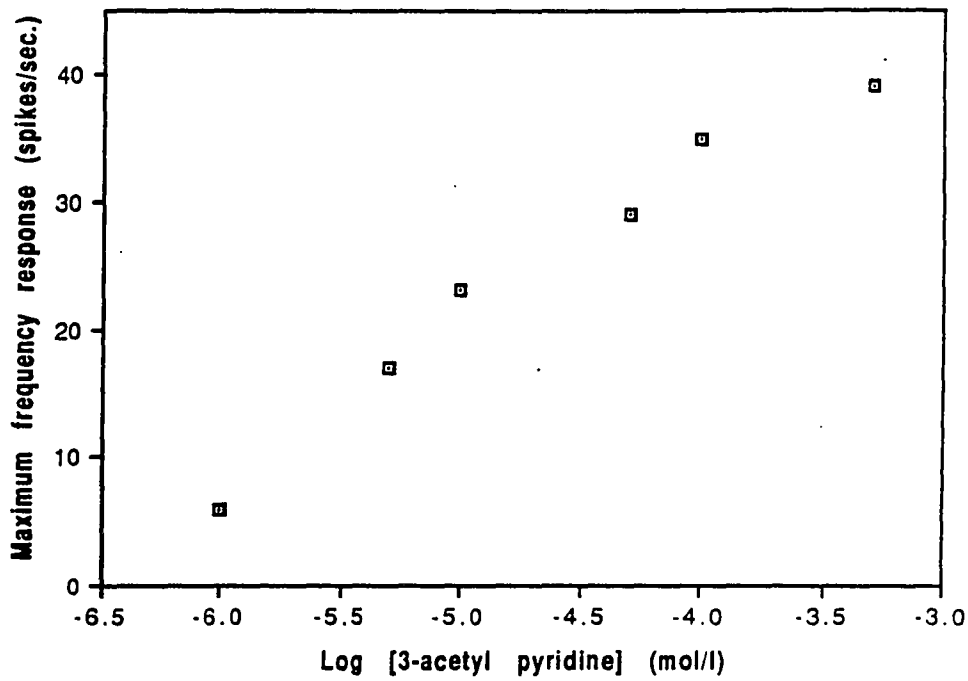

Figure 36. Single unit dose/response curve of the sensor to 3-acetyl pyridine.

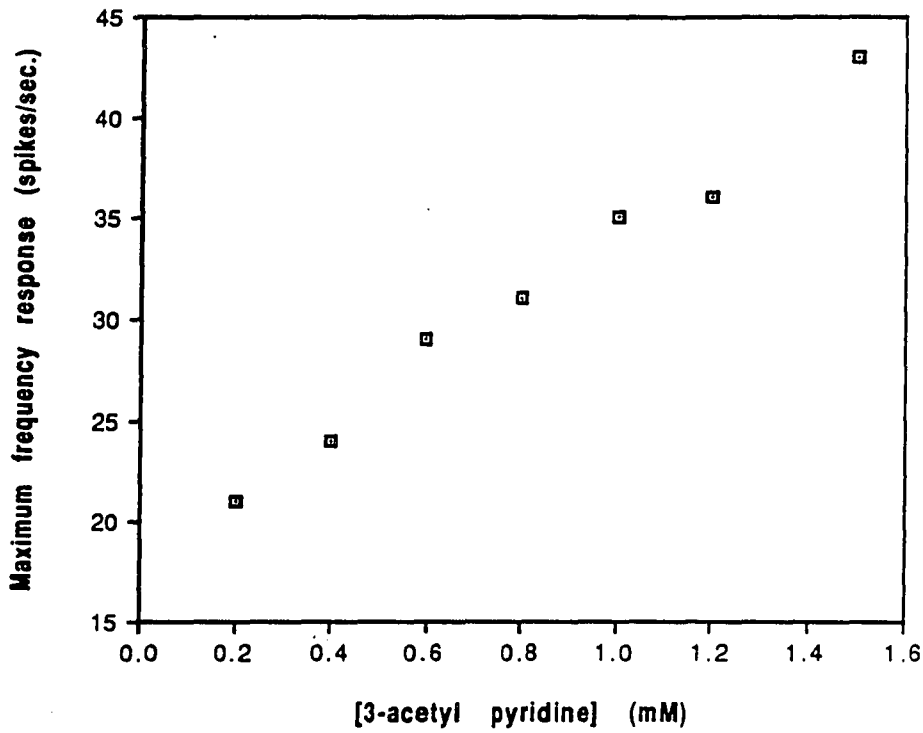

Figure 37. Dose/response relationship within a decade change in 3-acetyl pyridine concentration.

response times obtained with this novel sensor.

5.3.5 SELECTIVITY MEASUREMENTS

Over 15 different analytes were tested as possible stimulants with the antennule sensor. No analyte interfered with the primary stimulant, 3-acetyl pyridine, demonstrating the excellent selectivity of the sensor. However, crayfish antennular based sensor was used to detect another pyridine analog, pyrazinamide, as reported previously (109). The most important fact here is to fine tune the system until it produces a selective response.

5.3.6 LIFETIME STUDIES

Lifetime of excised crayfish antennules was monitored under different experimental conditions. It was found out that a saline solution saturated with oxygen could be used as a medium to extend the lifetime of excised antennules to over 6 days. However, excised antennules in saline solution showed a greater tendency to undergo moulting processes. Antennules at this stage could not be used to construct neuronal biosensors because of the softness of nerve tissues. The crayfish process of growth depends on moulting and the onset of moulting is under the control of an ecdysone hormone secreted by the Y-organ (114). The ecdysones are derived from cholesterol, which is a necessary part of the diet, as crayfish cannot synthesize this substance for themselves. In the intact intermoult animals the activity of the

Y-organ may be suppressed by the secretion of the so-called moult inhibiting hormone (MIH) from the X-organ, which is located in the eye stalk. Excised antennules have no such sources to release MIH and are therefore free to undergo moulting. Thus, hormonal functions are also important to prevent moulting, which is a severe restriction to extending the lifetime of crayfish antennules.

In order to extend the lifetime of neuronal sensors it would require a better understanding about the stability of exposed nerve cells under certain physiological conditions. However, the recent findings could be helpful in the future development of neuronal sensors with better long term stability.

CHAPTER 6
FUTURE DIRECTIONS

In the future, a further benefit may be expected from the video-assisted micromanipulation techniques proposed here. Specifically, it may become possible to connect the contact electrode directly to the stem of an individual aesthetasc (see figure 22) to prepare micro-scale receptrodes. Such an arrangement would also result in stronger and cleaner signals, perhaps with even greater selectivity, than the present sensors which rely upon electrical contact at the efferent neuronal fiber (fig. 24). Realization of this goal requires the use of contact micropipettes having diameters in the 1-2 micrometer range; Some technical problems associated with the use of such fragile probes are currently under investigation.

Although the lifetime of excised crayfish antennules was extended under certain conditions (low temperature, saline media) by about 18 times (over 6 days), dissected antennules cannot be kept alive more than 7-8 hours. An alternate approach would be to use the intact excised antennules (no dissection) to measure action potential spikes of nerve cells. This method essentially requires rigid microelectrode tips which can penetrate through the exoskeleton of the antennule.

Since each antennule has several thousand receptors, an array of microelectrodes could provide more informations than the single electrode set up. In this method, each microelectrode has to be

connected to separate amplifiers in order to amplify the potential signals. This approach is feasible only if microamplifier circuits can be build and coupled to the individual electrodes without gaining much noise. Rapid development of electronic technology would lead to the designing of such small electronic devices in the future.

Glass microelectrode techniques for measuring the action potential of nerve cells has a long history which extends back to the 1950 s. Two major drawbacks of this method are the insertion of electrode into the nerve cells (rather invasive) and also the inability to detect action potential signals from more than a few points simultaneously. Recent studies have demonstrated that a superconducting quantum interference device (SQUID) magnetometer can be used to measure the magnetic field associated with the electric currents of a propagating nerve action potential (115). However, the complexity of the system and also the requirement of liquid helium significantly limit the application of SQUID, although it provides the greatest possible signal-to-noise ratio. In order to avoid these difficulties Wikswo et al. (116) have recently developed a low-noise low-input impedance semiconductor amplifier which is adequately sensitive to allow detection of the magnetic field from isolated nerves. Application of magnetic field measurements will be a new direction for neuronal biosensor research in the future. This approach would facilitate to study different types of receptors simultaneously, similar to action potential measurements using a multielectrode set up. Chemometric data analysis methods can be used

to resolve the individual potential waves corresponding to stimulation from different analytes. Another possibility would be to measure the magnetic field from individual aesthetascs, which provide more selective and less complicated stimulant response patterns.

REFERENCES

(1) M.A. Arnold and M.E. Meyerhoff, CRC Critical Reviews in Analytical Chemistry, 20 (3) (1988) 149.

(2) G.A. Rechnitz, Chemical & Engineering News, 66 (1988) 24.

(3) L.C. Clark, Trans. Am. Soc. Artif. Internal Organs, 2 (1956) 41.

(4) L.C. Clark and L.C. Lyons, Ann. N.Y. Acad. Sci., 102 (1962) 29.

(5) G.A. Rechnitz, American Laboratory, 6 (2) (1974) 13.

(6) G.A. Rechnitz, Science, 190 (1975) 234.

(7) G.A. Rechnitz, Science, 214 (1981) 287.

(8) G.A. Rechnitz, T.L. Riechel, R.K. Kobos and M.E. Meyerhoff, Science, 199 (1978) 440.

(9) R.K. Kobos and G.A. Rechnitz, Anal. Lett., 10 (1978) 751.

(10) M.A. Jensen and G.A. Rechnitz, Anal. Chim. Acta, 101 (1978) 125.

(11) Chem. Eng. News, 56 (41) (1978) 16.

(12) G.A. Rechnitz, M.A. Arnorld and M.E. Meyerhoff, Nature (London), 278 (1979) 466.

(13) M. Mascini, M. Iannello and G. Palleschi, Anal. Chim. Acta, 138 (1982) 65.

(14) M. Aizawa, A. Morioka, S. Suzuki and Y. Nagamura, Anal. Biochemistry, 94 (1979) 22.

(15) S. Kuriyama and G.A. Rechnitz, Anal. Chim. Acta, 131 (1981) 91.

(16) J.S. Sidwell and G.A. Rechnitz, Biosensors, 2 (1986) 221.

(17) M.A. Arnold and G.A. Rechnitz, Biosensors, Fundamentals and Applications, Oxford University Press, (3) (1987) 30.

(18) H.F. Hameka and G.A. Rechnitz, J. Phys. Chem., 87 (1983) 1235.

(19) J. Wang and M.S. Lin, Anal. Chem., 60 (1988) 1545.

(20) A. Navaratne, M.S. Lin and G.A. Rechnitz, Anal. Chim. Acta, 237 (1990) 107.

(21) A. Navaratne and G.A. Rechnitz, Anal. Chim. Acta, (In Press).

(22) G.A. Rechnitz, Chem. Eng. News, 53 (4) (1975) 29.

(23) S.H. Synder, Science, 224 (1984) 22.

(24) L.B. Wingard Jr., Possibilities for Biosensors Based on Neuroreceptors, in Biosensors International Work shop, (ed. R.D. Schmid) VCH Publishers, Weinheim, (1987) 133.

(25) F. Hucho, Eur. J. Biochem., 158 (1986) 211.

(26) M.P. McCarthy, J.P. Earnest, E.F. Young, S. Choe and R.M. Stroud, Ann. Rev. Neurosci., 9 (1986) 383.

(27) R.W. Olsen, J. Yang, R.G. King and R.W. Ransom, Life Science, 39 (1986) 1969.

(28) S.F. Hallowell and G.A. Rechnitz, Anal. Lett., 20 (1987) 1929.

(29) M. Gotoh, E. Tamiya, M. Momoi and I. Karube, Anal. Lett., 20 (1987) 857.

(30) M.E. Eldefrawi, S.M. Sherby, A.G. Andreou, N.A. Mansour, Z. Annau, N.A. Blum and J.J. Valdes, Anal. Lett., 21 (1985) 1665.

(31) R.F. Taylor, I.G. Marenchic and E.J. Cook, Anal. Chim. Acta, 213 (1988) 131.

(32) K.R. Rogers, M.E. Eldefrawi and D.P. Richmann, Biosensor, Technology, Fundamentals and Applications, (ed. R.P. Buch, and M. Umena), Marcel Dekker, Inc., (1990) 383.

(33) M. Montal, R. Anholt and P. Labarca, The Reconstituted Acetylcholine Receptor, in Ion Channel Reconstitution, (ed. C. Miller), Plenum Press, New York, (1986) 157.

(34) R.M. Buch and G.A. Rechnitz, Anal. Chem., 61 (1989) 533A.

(35) Aspects of Chemoreception in Crustacea, Comp. Biochem. Physiolo., 8 (1963) 141.

(36) The Antennular Sense Organs of Crustacea, Comp. Biochem. Physiol., 13 (1964) 301.

(37) A. Kotyk, J. Bio-energ. Biomembr., 15 (1983) 307.

(38) V. Driessche and W. Zeiske, Physiol. Rev., 65 (1985) 833.

(39) E. Heinz, Mechanics and Energetics of Biological Transport, Springer, Berlin (1981).

(40) S.L. Belli and G.A. Rechnitz, Anal. Lett., 19 (3&4) (1986) 403.

(41) R.M. Buch and G.A. Rechnitz, Biosensors, 4 (1989) 215.

(42) R.M. Buch, T.Q. Barker and G.A. Rechnitz, Anal. Chim. Acta, 243 (1991) 157.

(43) B.W. Richardson, Lancet, 1 (1891) 707, 760.

(44) S.S. Wallian, N.Y. Med. J., 56 (1892) 594.

(45) W.C. Schumb, C.N. Satterfield and R.L. Weintworth, Hydrogen Peroxide, Reinhold Publishing Corporation, (1955) 615.

(46) S. Amberg, J. Biol. Chem., 1 (1906) 219.

(47 S. Anselmi, Ann. Chim. Applicata., 36 (1946) 321.

(48) J. Kisser and L. Portheim, Phytopath. Z., 7 (1934) 409.

(49) H.U. Bergmeyer and A. Hagen, Fresenius' Z. Anal. Chem., 261 (1972) 333.

(50) H.U. Bergmeyer and D. Jaworek, U.S. Pat., 3935071 (1976).

(51) M. Nelboeck and D. Jaworek, Chimia, 29 (1975) 109.

(52) W.C. Schumb, C.N. Satterfield and R.L. Wemtworth, Hydrogen Peroxide, Reinhold Publishing Corporation, (1955) 553.

(53) G.G. Guilbault and G.J. Lubrano, Anal. Chim. Acta, 64 (1973) 439.

(54) M.M. Fishman, Anal. Chem., 52 (1980) 185R.

(55) G.G. Guilbault, Analytical Uses of Immobilized Enzymes, Dekker, New York, (1984) 311.

(56) P.W. Carr and L.D. Bowers, Immobilized Enzymes in Analytical Chemistry and Clinical Chemistry, Wiley, New York, (1980) 241.

(57) J.E. Frew, M.A. Harmer, H.A.O. Hill and V.I. Libor, J. Electroanal. Chem. Interfacial Electrochem., 201 (1986) 1.

(58) M. Aizawa, I. Karube and S. Suzuki, Anal. Chim. Acta, 69 (1974) 431.

(59) M.A. Arnold and G.A. Rechnitz, Anal. Chem., 52 (1980) 1170.

(60) M.A. Arnold and G.A. Rechnitz, Anal. Chem., 53 (1981) 515.

(61) Zeile and Hellstrom, Hoppe-Seyl. Z., 192 (1930) 171.

(62) Keiilin and Hartree, Proc. Roy. Soc., B, 124 (1938) 397.

(63) S. Kumar, A. Singh and A.B. Abdi, Sci. Cult., 53 (1987) 381.

(64) G.G. Guilbault, Methods Enzymol., 44 (1976) 604.

(65) A. Ciucu, V. Magearu and C. Luca, Anal. Lett., 18 (B3) (1985) 299.

(66) B.C. Baldwin, Xenobiotic Metabolism in Plants. Drug Metabolism: From Microbe to Man (ed. D.V. Parke and R.L. Smith), Taylor and Francis, London, (1977) 191.

(67) J.R. Gillette, Fartschritte der Arzneimittelforschung, 6 (1963) 11.

(68) T.A. Smith, in Encyclopedia of Plant Physiology, (e.d. E.A. Bell and B.V. Charlwood), Springer Verlag, Berlin, 8 (1980) 433.

(69) T.A. Smith, Annu. Rev. Plant Physiology, 35 (1985a) 314.

(70) J.M. Hill and P.J.G. Mann, in Recent Aspects of Nitrogen Metabolism in Plants, (ed. E.J. Hewitt and C.V. Cutting), Academic Press, London, (1968) 149.

(71) E. Werle and D. Aures, Hoppe-Seyler's Z. Physiol. Chem., 326 (1961) 200.

(72) A. Rinaldi, G. Floris and B. Mondovi, Biochem. Biophys. Res. Commun., 155 (1983) 841.

(73) T.A. Smith, Annl. Biochem., 92 (1979) 331.

(74) R.K. Sindhu and H.V. Desai, Ind. J. Biochem. Biophys., 17 (1980) 194.

(75) D. Rudilier and G. Goas, Phytochemistry, 16 (1977) 509.

(76) A. Rinaldi, G. Floris, S. Sabatani and B. Mandovi, Bichem. Biophys. Res. Commun., 115 (1983) 841.

(77) T.A. Smith, Phytochemistry, 13 (1974) 1075.

(78) J.M. Hill, Methods Enzymol., 17B (1971) 730.

(79) S.K. Srivasatava and V. Prakash, Phytochemistry, 21 (1982) 1519.

(80) R. Price and R.L. Wain, Ann. Appl. Biol., 89 (1978) 485.

(81) R.J. Nash, T.A. Smith and R.L. Wain, Ann. Appl. Biol., 61 (1968) 481.

(82) R. Price, M. Albores and R.L Wain, Ann. Appl. Biol., 89 (1978) 479.

(83) J.M. Hill and P.J.G. Mann, Biochem. J., 91 (1964) 171.

(84) A.W. Andreae, Nature, 175 (1955) 859.

(85) R.H. Kenten and P.J.G. Mann, Biochem, 50 (1952) 360.

(86) D. Wijesuriya, M.S. Lin and G.A. Rechnitz, Anal. Chim. Acta, 234 (1990) 453.

(87) A. Navaratne, M.S. Lin and G.A. Rechnitz, Anal. Chim. Acta., (1990) (In Press).

(88) Leydig, Das Auge der Gliederthiere, (1964)

(89) H. Hatt and I. Scemiedel-Jakob, J. Comp. Physiology, A, 1545 (1984) 855.

(90) H.J. Takken, L.M. Vander Linde, M. Boelens and J. van Dort, J. Agric. Food Chem., 23 (1975) 638.

(91) J.W. Wheeler and M.S. Blum, Science, 182 (1973) 501.

(92) R.M. Seifert, R.G. Buttery, D.G. Guadaginis and J.G. Harris, J. Agric. Food Chem., 20 (1972) 135.

(93) H.D. Belitz, W. Chen, H. Jugel, R. Treleano and H. Wiser, Sweet and Bitter Compounds: Structure and Taste Relationship. In: Boudreau JC (ed) Food Taste Chemistry, ACS Symp. Ser., 115 (1979) 93.

(94) G.E. Loeb, M.J. Bak, M. Salcman and E. Schmidt, IEEE Tran. Biomed. Eng., BME-24, (1977) 121.

(95) K. Frank and M.C. Becker, Microelectrodes for Recording and Stimulation, in Physical Techniques in Biological Reserach, (ed. W. Nastuk), Academic, New York, Part A, 5 (1964) 22.

(96) R.L Schoenfeld, Bioelectric Amplifiers, In Physical Techniques in Biological Research. (ed. W. Nastuk), Academic, New York, V (1964) 277.

(97) M. Armstrong and J. Millar, J. Neurosci. Methods, 1 (1979) 279.

(98) K. Fox, M. Armstrong and J. Millar, J. Neurosci. Methods, 3 (1980) 37.

(99) C.W. Anderson and M. Cushman, J. Neurosci. Methods, 4 (1981) 435.

(100) R.S. Pickard, Trends Neurosci., 2 (1979a) 259.

(101) R.S. Pickard, J. Neurosci. Methods, 1 (1979b) 301.

(102) D.M. Holdich and R.S. Lowery, Freshwater Crayfisy, Biology,

Management and Exploitation, The University Press, Cambridge, (1983) 13.

(103) E.S. Hodgson, Biol. Bull., (Wood's Hole) 115 (1958) 114.

(104) W.S. Thomas, J. Zool., 160 (1970) 91.

(105) C. Ameyaw-Akumfic, Crustaceana, 33 (1977) 259.

(106) H. Hatt, J. Comp. Physiology, 152 (1983) 405.

(107) R.M. Buch and G.A. Rechnitz, Anal. Lett., 22 (13&14) (1989) 2685.

(108) T.Q. Barker, R.M. Buch and G.A. Rechnitz, Biotechnol. Prog., 6 (1990) 498.

(109) D. Wijesuriya and G.A. Rechnitz, Anal. Chim. Acta, (1992) In Press.

(110) J.C. Desclin and J. Escubi, Brain Research, 77 (1974) 349.

(111) C.B. Balaban, Brain Research Rev., 9 (1985) 21.

(112) R. Linas, K. Walton, D.E. Hillman and C. Sotelo, Science, 190 (1975) 1230.

(113) A. Sydney, Chem. Abstract, 112 (1990) 579 (35839p).

(114) D.M Holdich and R.S. Lowery, Freshwater Crayfish , Biology, Management and Exploitation, The University Press, Cambridge, (1983) 83.

(115) J.P. Wikswo, Rev. Sci. Inst., 53 (12) (1982) 1846.

(116) J.P. Wikswo, P.C. Samson and R. Giffard, IEEE Trans. Biomed. Eng., BME-30, 4 (1983) 215.